ANL-6565

ANL-6565

Argonne National Laboratory

REACTOR DEVELOPMENT PROGRAM

PROGRESS REPORT

April 1962

ANL-6565
Reactor Technology
(TID-4500, 17th Ed.)
AEC Research and
Development Report

ARGONNE NATIONAL LABORATORY
9700 South Cass Avenue
Argonne, Illinois

REACTOR DEVELOPMENT PROGRAM PROGRESS REPORT

April 1962

Albert V. Crewe, Laboratory Director

Division	Director
Chemical Engineering	S. Lawroski
Idaho	M. Novick
Metallurgy	F. G. Foote
Reactor Engineering	B. I. Spinrad
Remote Control	R. C. Goertz

- - - - -

Report coordinated by R. M. Adams

Issued May 15, 1962

Operated by The University of Chicago
under
Contract W-31-109-eng-38

FOREWORD

The Reactor Development Program Progress Report, issued monthly, is intended to be a means of reporting those items of significant technical progress which have occurred in both the specific reactor projects and the general engineering research and development programs. The report is organized in a way which, it is hoped, gives the clearest, most logical over-all view of progress. The budget classification is followed only in broad outline, and no attempt is made to report separately on each sub-activity number. Further, since the intent is to report only items of significant progress, not all activities are reported each month. In order to issue this report as soon as possible after the end of the month editorial work must necessarily be limited. Also, since this is an informal progress report, the results and data presented should be understood to be preliminary and subject to change unless otherwise stated.

The issuance of these reports is not intended to constitute publication in any sense of the word. Final results either will be submitted for publication in regular professional journals or will be published in the form of ANL topical reports.

The last six reports issued
in this series are:

October 1961	ANL-6454
November 1961	ANL-6473
December 1961	ANL-6485
January 1962	ANL-6509
February 1962	ANL-6525
March 1962	ANL-6544

TABLE OF CONTENTS

TABLE OF CONTENTS

I. WATER COOLED REACTORS

A. General Research and Development

1. Fuel Development - Irradiation Studies

A three-rod prototype fuel element consisting of UO_2 pellets in collapsed A-288 aluminum alloy tubing removed some time ago from the ANL-2 High Pressure Water Loop at MTR (see Progress Report, October 1961, ANL-6454), is undergoing a hot cell examination. Designation of the element is ANL-2-13. Each of the three rods in the element is 16 in. long and contains a column of UO_2 pellets (0.321 in. diameter, 3.05% enriched) which have a density 95% of theoretical. The wrought A-288 aluminum alloy (1 w/o Ni, 0.5 w/o Fe, 0.1 w/o Ti, $<$20 ppm Si) tubing used for cladding has an O.D. of 0.385 in. with a wall thickness of 0.030 in. One rod contains square end pellets with a 0.001 in. thick annular gap filled with helium. Another rod contains square end pellets with zero gap prior to irradiation. This was accomplished by hydrostatically collapsing the tube on the pellets before irradiation. The third rod contains pellets with dished ends and an annular helium-filled gap 0.001 in. thick.

During the three months that the element was under irradiation no fission product activity or other difficulty appeared. The hot laboratory examination now in progress has also indicated that the element operated without difficulty. The following observations have been made to date:

The rod which contained square end pellets had elongated 0.021 in. The rod which contained square end pellets and which had been subjected to high external pressure prior to irradiation to ensure cladding collapse had elongated 0.015 in. The rod which contained pellets with dished ends had elongated 0.005 in.

Scale deposition approximately 0.002 in. thick was present on the entire assembly. The scale was colored a hematite-red, and is presumably largely composed of iron oxide that resulted from corrosion of the stainless steel loop. The scale was most tightly adherent on the surface of the cladding where local boiling had occurred.

The rod with square end pellets and which elongated 0.021 in. showed some bulging where temperatures were highest. This is believed to have resulted from restraint of axial thermal expansion. The rod had shifted in its holder evidently at some time early in the experiment, so that the hot end of the rod could not expand freely.

The results obtained thus far indicate that ratcheting did not occur between the fuel pellets and the aluminum alloy cladding, particularly in the rod containing pellets with dished ends. It would therefore appear that

serious consideration can be given to the use of wrought aluminum alloy tubing as a cladding material for UO_2 pellets in water reactors and also quite likely, in organic-cooled reactors. The use of the more expensive sintered aluminum powder product tubing in order to have free-standing pellets does not appear to be essential.

2. Heat Engineering

The influence of voids in the downcomer of a boiling water reactor was studied in connection with the spectral-shift concept of reactor operation. The coolant velocity is reduced by the introduction of voids in the downcomer and at the core inlet. Calculations show there is a 30% reduction in the coolant velocity in a system having a void fraction of 0.2 in both the downcomer and in the inlet plenum and a void fraction of 0.6 in the core exit fluid when compared to a system having zero void fractions in the downcomer and inlet plenum and a void fraction of 0.4 in the core exit fluid. The lower coolant velocity results in reduced power output of the reactor. A study will be made to compare and evaluate the disadvantages resulting from the reduction in power with the advantages, such as achieving more uniform fuel burnup and simpler control.

3. Instrumentation

The Laboratory is conducting evaluation tests at the request of the AEC on two ultrasonic transducers. The tests were to determine the ability of the transducers to detect steam-water interface levels and to determine reliability of operation under temperature and nuclear environment.

The two ultrasonic level transducers were found to be leaky and were sent back to the manufacturer some time ago (see ANL-6269, Progress Report, November, 1960). The manufacturer has returned the transducers for further testing. The preparatory test work reveals that it is necessary to provide seals to prevent moisture from entering the magnesium oxide cable. In addition, one of the transducers appears to have a questionable weld between the signal cable sheath and the transducer body. This weld will be examined by X-ray.

B. EBWR

1. Reactor Component Examinations

a. 17-4 PH Components - The 17-4 PH, H-1100 rack, pinion shaft, and seal shaft on Control Rod No. 3 were removed for routine examination by magnaglow and dye penetrant techniques. No flaws were discovered in the 17-4 PH material but cracks were found in the $\frac{3}{16}$-in. diameter Type 420 stainless steel roll pin. The pin connects the pinion shaft to the drive shaft at a splined coupling. The lateral removal of this shafting disengages

the pinion gear from the rack which is fixed to the control rod and follower. This design feature permits the control rod to be dropped back into the core in case malfunctions occur in the linkages between the motor drive and the rack.

The pins in the other eight drives were examined and four were found to be cracked. An investigation is being made to determine the cause of failure in the pins. In the interim, the pin holes in the male spline of the pinion shafts were increased in diameter to assure that the spline and not the pin transmits the rotation forces.

b. Control Rods - The No. 3 boron-stainless steel and the No. 9 hafnium control rods were raised to the top of the water-filled reactor vessel and examined visually under high intensity light with a mirror and a low power periscope. Spotwelds, rivets, and angle bends were scrutinized in particular detail and no flaws were discovered in these components.

c. Burnable Poison Strip - An irradiated 1.1% boron-stainless steel strip was removed for examination from a fuel element spike after being exposed in the reactor for a total of 6325 Mw-hr.

The results of the examination are summarized:

(1) The tack welds holding the strip to the frame were physically sound.

(2) No defects such as tears, cracks, etc., were observed.

(3) Some brown crud was noted on the strip, probably ferric oxide.

(4) The boron strip is still ductile to a 100-degree bend.

(5) The expected burnup of boron in the strip is not entirely corroborated by the lithium analysis.

The strip was scanned with a gamma ray detector and the results are shown in Figure 1. This survey provides an approximate axial pattern of the flux. The unirradiated sample data is an analysis of material from the same heat as the irradiated samples. The irradiated samples are identified in Figure 1. Boron and lithium analyses were made on samples 1, 2, and 3. The results are shown in Table I. Two bend tests were made on samples A and C and one on B. These data are shown in Table II. From the bend tests it can be noted that the material in location C has lost some of its ductility while the material in sections A and B has retained the ductility of the unirradiated material.

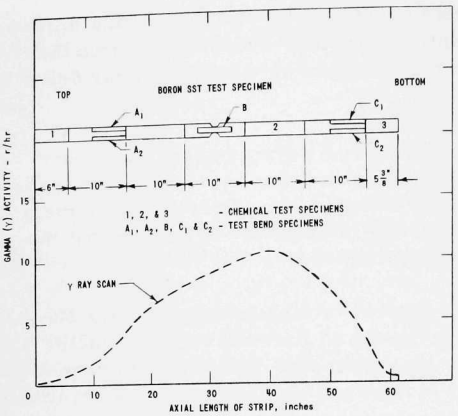

Figure 1

A Scan of Gamma (γ) Activity Level of a Boron Strip Removed from EBWR Irradiated Spike Fuel Element

Table I. Boron and Lithium Analyses

Sample	Boron Content, (wt-%)	Lithium Content, (wt-%)
Unirradiated	1.27/1.29	0
1	1.16/1.18	0.031
2	1.21/1.23	0.047
3	1.26/1.29	0.018

Table II. Bend Test Data

Sample	Angle (degrees)	Force* (lb)	Remarks
Unirradiated	100	Not measured	No cracks.
	180		Began to crack at edges.
A_1	100	152	No cracks.
	180		Began to crack at edges.
A_2	100	149	No cracks.
	180		Began to crack at edges.
B	100	174	No cracks.
	190		Small cracks on edges.
C_1	100	162	No cracks.
	160		Sample broke in two.
C_2	100	152	No cracks.
	110		Sample broke in two.

*Pin diameter for all bends is $\frac{1}{2}$ in.

Thickness measurements of unirradiated strips ranged from 0.060 in. to 0.062 in. The irradiated strip ranged in thickness from 0.060 in. to 0.064 in. This small deviation could be due to the film of crud or to the rolling tolerances.

2. EBWR Soluble Poison Control System - 100-Mw Operation

The soluble poison addition system has been found adequate to provide holddown and shim control for 100-Mw operation. The addition pumps have been calibrated for reactor pressures to 600 psig. The pumping rate of the two fixed speed units, operated from the EBWR Control Room, exceeds the design specifications of 2.87 gpm up to 300 psi, and effectively equals the specified rate of 2.83 gpm at 600 psig. In addition a variable rate pump provided specifically for use during filling operations was also calibrated.

The neutron attenuation instrument for monitoring the soluble poison concentration in EBWR water has undergone improvement and evaluation. The manual monitor, using a 1.25×10^6 n/sec plutonium-beryllium source, has been particularly reliable in performance. The continuous monitor has been modified from the original design described in ANL-6439* to improve long-term stability and facilitate periodic maintenance and calibration.

The purification (removal of soluble poison) system is still undergoing study and evaluation to determine optimum operating parameters for use at the higher power levels.

3. EBWR Control Rod Calibration

The present core of EBWR has been loaded with 32 spikes, 28 of which are located in the ring just outside the control rods. The spikes have an average of 1.57 poison strips per spike.

With the present loading of the reactor, and with its new set of control rods with Zircaloy followers, the reactor is capable of meeting the cold shutdown requirements specified in the Hazards Summary Report, ANL-5781-Addendum (Rev. 1). It has been estimated also, that there is sufficient reactivity in the core to enable the reactor to go to 80 Mw, and possibly up to 100 Mw if favorable hydrodynamic conditions prevail.

Two additional calibrations were made for the new set of control rods. The poison section of rods Nos. 1-8 consist of heat treated 2 wt-% boron-stainless steel alloy and rod No. 9 is made of hafnium. All rods have Zircaloy followers. One calibration was made using all rods in bank control and the second calibration was made with the central rod, No. 9, moved with respect to the balance of the rods, No. 1-8, moved as a bank. The data are currently being analyzed.

* Roland J. Armani, "The Continuous Monitoring of Boric Acid Concentration by Neutron Absorptiometry," ANL-6439 (October, 1961).

4. Plutonium Recycle Study

A study of plutonium recycle reactor systems has been initiated. The objective of the study is to define a program to be carried out with the EBWR reactor which would be useful in the development of plutonium recycle systems. The study naturally falls into two phases:

(1) to specify one or more promising full-scale recycle systems and to determine the characteristics and relative merits of these systems

(2) to define an EBWR program which will be useful in the above specified systems.

The initial efforts will be restricted to the first phase and will be further oriented to the possible use of a fast and thermal reactor complex in which the two reactors are coupled through fuel exchange (e.g., the fuel bred in the fast reactor blanket will be used, without reprocessing, as fuel for the thermal reactor, and the processed fuel after introduction in the thermal reactor will be used as makeup material for the fast core).

C. BORAX-V

1. Operations and Experiments

Experiments were performed with the reactor loaded with 60 boiling fuel assemblies, each with forty-nine 5%-enriched fuel rods, except for 36 boron-stainless steel rods substituted for fuel rods. A total of 35 kg of boric acid was dissolved in the reactor water to compensate for excess reactivity so that control rods could be withdrawn to calibrate their reactivity worth. The total control rod worth was found to be about 19% $\Delta k/k$. The total excess reactivity available in the cold clean reactor is 12% $\Delta k/k$, and the shutdown margin under these conditions is 7% $\Delta k/k$.

Substitutions were made with this core loading poisoned with boric acid as a reference. Boron-stainless steel poison rods were substituted for fuel rods in three positions denoted by the letters "a," "b," and "c" in Figure 2. The resulting reactivity changes were, -0.09, -0.09 and -0.049% $\Delta k/k$ per rod, respectively. The net effect of the boron in one of these rods in position "a" was found to be -0.065% $\Delta k/k$ per rod. This was determined by comparing the effect of stainless steel rods with the effect of boron-stainless steel rods. Substitution of water rods for fuel rods in the "a" position made a very slight negative change. The water rods are hollow aluminum tubes which fill with the water in the reactor containing boric acid in this case.

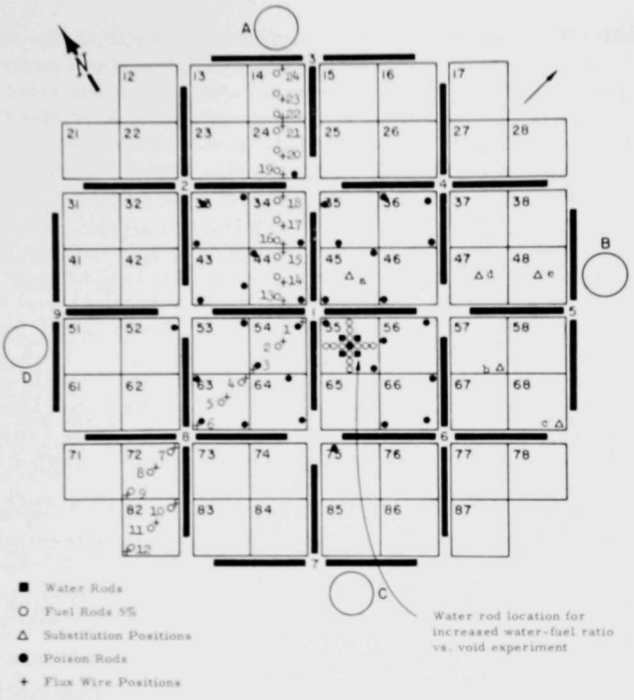

Figure 2. Experimental Loading Diagram-Boiling Core BORAX-V

Substituting 10%-enriched for 5%-enriched fuel rods in the positions marked "a," "d," and "e" on Figure 2 resulted in reactivity changes of +0.011, +0.006, and +0.003% $\Delta k/k$ per rod.

The effect of changing temperature from 79 to 112°F at the boric acid concentration of 18.75 gm/gallon is about +.047% $\Delta k/k$. When the correction is made for the net change of boric acid resulting from the expansion of water and the core structure, the reactivity effect from the temperature change is essentially zero.

The reactivity worths of simulated voids in the moderator were measured at room temperature on the boiling core poisoned with boric acid. To make the measurements, aluminum void tubes were compared with water-filled tubes in the coolant channels and upper reflector of the boiling fuel assemblies. The average value for the reactivity worth of boric acid solution throughout the core was used to correct the void worth measurements for the effect of displaced boric acid.

With 120 void tubes, representing about 0.5 v/o of the water in the core, uniformly distributed throughout the core, the upper reflector and the upper two inches of the lower reflector, the void coefficient was measured to be -0.36% $\Delta k/k/\%$ void. The same amount of void distributed non-uniformly to simulate an actual boiling core void distribution gave a void coefficient of about -0.45% $\Delta k/k/\%$ void. With the same void uniformly distributed through the central 16 fuel assemblies only, the coefficient was measured to be roughly -0.55% $\Delta k/k/\%$ void.

To determine the effect of increased water-fuel ratio on the reactivity worth of voids, the five fuel rods in the central 16 fuel assemblies only, located as shown in Figure 2, were replaced with water rods. This changes the $H_2O - U^{235}$ weight ratio in these assemblies from 4.99 in the reference core to 5.73, an increase of 14.8%. The void worth with the increased water-fuel ratio was approximately one-half the value measured for the reference core ratio. The change in available excess reactivity due to the substitution of water rods for fuel rods was -0.44% $\Delta k/k$.

As reported in ANL-6302,* the calculated worth of voids distributed only in the core at room temperature, not considering streaming through the upper and lower reflector, was -0.21% $\Delta k/k/\%$ void. To check the calculational techniques used, additional problems have been prepared using the same parameters (including boric acid) as in the above void worth measurements.

Flux wire irradiations were made to obtain detailed and overall thermal flux distributions and cadmium ratios. Using $3\frac{1}{2}\%$ U^{235}-Zr alloy and gold wires, both bare and cadmium-covered, results obtained from short wires ($\frac{3}{8}$ in. in length) are being compared with results using 36-in. long wires to check the beta counting efficiency of the automatic flux wire scanner. Figure 3 shows typical radial flux patterns for the boiling core measured in the positions shown on Figure 2.

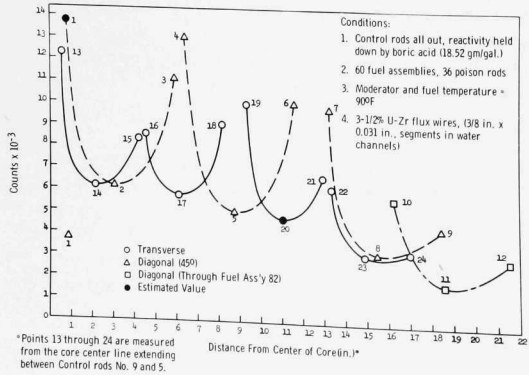

Figure 3

BORAX-V Radial Flux Plot at Axial Midplane

*R. E. Rice, et al, Design and Hazards Summary Report (BORAX-V) May, 1961.

Measurements are also being made in $\frac{1}{8}$ in. O.D. stainless steel thimbles to simulate the flux measurements to be made at power with the flux wires in pressure thimbles and to obtain the effect of the stainless steel thimbles on Cd-ratio.

Fine flux mapping of one octant of the core was concluded. Uranium-Zr wires were held adjacent to fuel rods within a fuel assembly by means of a polyethylene block which was pierced by the fuel rods. Proper locations for poison rods, water rods and 10%-enriched fuel rods will be determined upon analysis of the flux plots.

A comparison of a standard fuel assembly at the center of the core, with one containing five water rods instead of fuel rods in the center of the assembly, has been made using fine flux plots. The peak flux levels were normalized, and the power production in the assembly with water rods was only about 2% less in spite of having 10% fewer fuel rods. The peak-to-average flux level in the assembly dropped from 1.44 to 1.27 when the water rods were added.

2. Production and Fabrication

a. Superheat Core - Production fuel plates required under provisions of the Atomics International contract contain either depleted UO_2 (types HCD, FCD, HPD, and FPD) or enriched UO_2 (types HCE, FCE, HPE, and FPE). All fuel plates containing depleted UO_2 have been received from AI, inspected and accepted by ANL. All required fuel plates containing enriched UO_2 have also been received. Inspection of these enriched plates is currently being performed.

Of the original 190 type HCE plates received, two were rejected. Replacements for these two rejected plates have subsequently been received from AI, and upon evaluation were found to be acceptable. No additional type HCE plates are required under the contract provisions. The 190 type FCE plates which were supplied by AI have been inspected and all except five have been accepted. The five rejected plates are to be replaced.

A total of 138 type HPE plates have been completely evaluated. Only one of these has been rejected to date. Except for the nondestructive test for bond integrity, all of the type FPE plates have been inspected. Ultrasonic through transmission testing and tabulation of all other inspection data, on remaining type HPE and type FPE plates, is continuing.

Another group of five developmental superheater fuel elements was assembled and vacuum brazed. Two of the elements were composed of depleted peripheral type plates, and three elements were assembled using solid stainless steel plates instead of fuel plates. The procedures which were varied in the assembly and brazing of these elements are shown in Table III.

Table III. Developmental Superheater Fuel Elements

	Braze Alloy Application	Plate Surface Preparation	Furnace Position
Fuel Element 1	Sides & Tops of Spacer Wires	HNO_3-HF Pickled HNO_3 Psssivated Cold Finished	Horizontal
Fuel Element 2	Sides & Tops of Spacer Wires	HNO_3-HF Pickled HNO_3 Passivated Cold Finished	Horizontal
Dummy Element 1	Sides & Tops of Spacer Wires	HNO_3-HF Pickled HNO_3 Passivated	Horizontal
Dummy Element 2	Sides of Spacer Wires Only	As Rolled	Horizontal
Dummy Element 3	One Side of Spacer Wires	As Rolled	Vertical (on edge)

Destructive examination of these elements was carried out to determine the success of the brazing operation. The degree and adequacy of bonding in dummy elements 2 and 3 was much greater than for the other three elements. It appears that in the two satisfactorily brazed elements, the braze alloy remained near the joint areas and was available to produce a sound bond between adjoining parts. The alloy was spread out more thinly and completely over the plate surfaces in the other three elements and, consequently, not enough was available at junction locations to achieve thorough bonding.

These results indicate that the surface condition of the fuel plates affects the extent of flowing or spreading of the braze alloy. In order to test this hypothesis, several 3-inch-square, thin stainless steel plates were subjected to various surface treatments. Braze alloy was then applied in equal amounts to each sample and the samples were subjected to the standard vacuum brazing cycle. The results obtained are shown in Table IV.

Since the pickled, passivated, and wire brushed sample gave the most desirable results, the surfaces of four depleted peripheral plates were wire brushed. After assembly and vacuum brazing, the depleted element was sectioned for destructive examination and was found to be satisfactorily brazed. One piece approximately 12 in. long was subjected to a hydrostatic pressure test. Failure occurred within the fuel plates rather than at the brazed joints.

Table IV. Effect of Surface Preparation on Flow of Braze Alloy

Sample Number	Surface Preparation	Extent of Flow (Relative Position)
1	As stocked	3
2	HNO_3-HF pickled	5
3	HNO_3-HF pickled HNO_3 passivated	6
4	HNO_3-HF pickled HNO_3 passivated Heated in air to 800°F	4
5	HNO_3-HF pickled HNO_3 passivated Wire brushed	1 (least flow)
6	HNO_3-HF pickled HNO_3 passivated Steel wool abraded	2
7	HNO_3-HF pickled HNO_3 passivated Sand blasted	7 (most flow)

The surfaces of 20 more depleted plates were prepared for brazing by stainless steel wire brushing and stainless steel wool abrading. Since not enough production depleted fuel plates were available for five elements, a group of rejected, depleted plates was used. After assembly, three of the elements were brazed at 2150°F and two at 2100°F. Metallographic examination and hydrostatic pressure testing, indicated that the brazed joints are satisfactory, but that the 2150°F brazing temperature is superior. Corrosion tests were run in water at 315°C and in steam at 650°C on samples of wire-brushed, depleted plates to determine if wire brushing of the Type 304L stainless steel surface affected the corrosion resistance of the material. The samples tested in 315°C water indicated satisfactory corrosion resistance after 144 hours and the 650°C test is still continuing.

Metallographic examination of end and center sections from each of the last six elements brazed has been performed. Spacer wire-to-plate joints have been satisfactorily bonded in all cases. It should be kept in mind, however, that porosity and incompletely filled side plate channels have been found to some degree in every element produced thus far.

b. Reactor Components - Fabrication of eleven Type 304L stainless steel clad poison sections of the new control rods was completed. The rods were helium leak tested, dye penetrant tested, and then autoclave tested for seven days at 600 psig, 486°F conditions. No indication of leaks or swelling in the rods was found, but the cladding between slugs in the gas expansion space region was dished slightly. The poison sections have been straightened (they had not previously been straightened) and reinstalled in the autoclave for additional testing. The X-8001 aluminum follower and stainless steel cruciform extension portions of these rods are complete and ready for assembly.

Ten 17-4 PH, chrome-plated, stainless steel control rod extension shafts have been delivered to the reactor site. One spare shaft is being fabricated.

The dummy control rod with the new design of follower-to-cruciform extension mechanical joint has been scrammed 1,000 times at 600 psig, 486°F conditions with no damage to the joint or rod.

3. Development and Testing

a. Plant Tests - The experiments with a boiling core using boric acid are still proceeding. A system for dissolving, injecting, and sampling boric acid was assembled and used for this work. During this period 51 samples of the boric acid solution in the reactor vessel were analyzed for boric acid concentration. This involved performance of 105 separate determinations. Over sixty more samples were taken for storage in case check results were desired. Sampling at the top, the middle, and the bottom of the reactor vessel showed that mixing for one hour with the auxiliary pump gave a completely homogeneous solution. After this was established, all further samples were taken just at the top of the reactor core.

b. Water Chemistry Tests - Tests of Polybor - The preliminary pH control, aluminum corrosion, and demineralization test on Polybor (disodium-octaborate) were completed. In a previous report, it was stated, tentatively, that a boron-containing gas was given off during the demineralization tests. This gas was subsequently identified as CO_2 and the boron indication was found to be spurious. The CO_2 was given off because the ion-exchange resin used had been exposed to air for a long period prior to its use in the tests. It was found that Polybor or a mixture of Polybor-boric acid can successfully be removed from solution using a mixed bed ion-exchange resin containing strong anion and cation resins.

The pH control tests showed that boric acid can be used to lower the pH of Polybor solutions.

The corrosion tests on aluminum (X-8001) and 304 stainless steel sample couples in Polybor and Polybor-boric acid solutions at 700 psig saturated conditions showed that a reactor shutdown using these solutions could permanently and seriously damage a reactor having aluminum fuel cladding or structural parts. Because the corrosion tests were performed before measured data on boron worth had been obtained from BORAX V, the concentrations used in these tests were found to be roughly $4\frac{1}{2}$ times the concentrations needed to shut down BORAX V. After the tests, the stainless steel samples were lightly coated with α-aluminum oxide or boehmite. The aluminum samples were thickly coated with two layers of very adherent boehmite. A heavy (1-2 mils) black, brittle layer was found adjacent to the metal. This was covered by a white crust of the same stoichiometric composition. The coating was adherent and neither layer was removed by 60 hours of soaking in room temperature water. An analysis of the two layers showed that the black layer contained approximately 3.5% boron by weight and the white layer approximately 0.5% boron. The black layer contained 5% iron which probably was present as magnetite and accounts for its black color.

During the autoclaving of the samples in the Polybor solutions, pressure gages showed wide variations above the saturation value given by steam tables for the test temperature. The pressure was cycled at varying rates during the entire test period and after cooling the autoclaves, a residual pressure of about 300 lb remained. No means of sampling was available, hence the gas could not be identified; tentatively, however, it is thought to be hydrogen from reaction of the aluminum with the Polybor solution.

Further tests are planned using much more dilute solutions, taps for gas samples, and pressure transducers and recorders to obtain a record of the gas generation and reabsorption behavior.

c. Recombiner Tests - Results of corrosion test on samples of Type 304 stainless steel in highly oxygenated superheated steam of 1200°F by ANL and others indicate that the high oxygen content of the steam is conducive to severe surface oxidation and spalling and to chloride stress corrosion. Therefore, it is deemed desirable to reduce or neutralize the amount of oxygen in the saturated steam from the boiling zone of the reactor before it enters the superheater. The oxygen might be reduced either by catalytic recombination or by continuous addition of H_2 gas to the reactor water.

A test rig for determining the feasibility of effective recombination of the radiolytically formed free H_2 and O_2 gas by means of a platinized demister pad in the reactor vessel steam dome has been built.

Preliminary shakedown steaming runs on this equipment have been accomplished this month to check instrumentation, head loss through the demister and performance. Several modifications have been made to improve steam flow conditions and steam-water separation.

d. Corrosion of Structural Materials in Superheated Steam - There has been no change in behavior of the previously discussed materials in oxygenated superheated steam at 650°C and 600 psi.

In addition to these materials, Inconel and Croloy $2\frac{1}{4}$ (low alloy steel) have been tested. Inconel samples, with a variety of surface treatments, exhibited adherent films and a low corrosion rate which decreases with time. Croloy $2\frac{1}{4}$ had a very high weight gain (~3500 mg/dm^2) after 7 days.

Additional samples of Type 304 subjected to various chemical surface treatments showed the severe spalling found to be typical in the initial exposure periods.

II. LIQUID METAL COOLED REACTORS

A. General Research and Development

1. ZPR-III

a. Experimental - In continuation of the critical studies of shape effect, Assembly 39 was constructed in ZPR-III. This is a spherical version of Assembly 31, a cylinder whose composition simulated a metallic, low-density uranium fueled core with a high-density, depleted uranium blanket. Thus Assemblies 39 and 31 form a set similar in size to the previous 38 (spherical) and 24 (cylindrical). The set 39 and 31 have composition which corresponds to reactor No. 3 of Loewenstein and Main's shape factor studies, ANL-6403, except for the substitution of sodium for aluminum. The set 38 and 24 correspond rather closely to the composition of Loewenstein and Main's reactor No. 1, a high-density, metallic uranium core. Thus several experimental check points are now available for comparison with ANL-6403. The critical mass of Assembly 39 has now been found to be 426.7 kg U^{235}.

It is understood that several improvements in the calculations of ANL-6403 have been effected since publication, so that any comparison made now between the experiment and published values may be subject to revision. However, Table V is presented here to give some tentative comparisons. In Table V the estimated maximum shape factors are those where the curve of shape factor versus L/D reaches its peak. In ANL-6403 these values are obtained as a result of a series of calculations at different L/D values.

Table V. Experimental and Calculated Shape Factors

			Shape Factor			
			Experimental		Calculated	
Ass'y	Shape	Core Type	Observed	Est. Max.	Calc.	Est. Max.
38	Sphere	High Density	0.920	0.920	0.99	0.99
24	Cylinder, L/D = 0.93	High Density				
39	Sphere	Low Density	0.922	0.932	0.92	0.93
31	Cylinder, L/D = 0.73	Low Density				

In the experimental case, only one L/D ratio was studied at each composition, and therefore the experimental estimated maximum is obtained by assuming that the calculated curve shape is correct with perhaps some overall displacement.

The experiments are performed on systems having a certain degree of heterogeneity, being composed of $\frac{1}{8}$ in. plates. They are also subject to uncertainties due to the necessity of approximating curved shapes with a rectangular module. These uncertainties are small and in addition, are expected to be fairly constant throughout the whole series of experiments. With these minor reservations, the conclusion from the experimental results is that the core density has less effect on shape factor than the calculations seemed to indicate.

Experiments are continuing on Assembly 39 to obtain flux traverses, particularly to determine if the heterogeneity of the materials introduces major anisotropies in the buckling.

b. Theoretical - It has been usual in calculations of ZPR-III cylindrical assemblies to use estimated shape factors to convert calculated spherical masses to cylindrical critical masses. Shape factors based upon Figure 6-2 in ANL-5800 (Reactor Physics Constants) have generally been used.

To estimate the extent that uncertainty in shape factors may be responsible for discrepancies between experimental and calculated critical masses three assemblies have been calculated using a two-dimensional transport code in x-z geometry. The Los Alamos TDC code in the S_4 approximation was used with two energy groups having lower energy limits of 1.35 Mev and 9.12 kev. The corresponding spherical cases were calculated using the Los Alamos DSN code in the S_4 approximation. The assemblies studied are Nos. 23, 32, and 31 which are each fueled with U^{235} and have as diluents aluminum, steel, and aluminum and steel, respectively. These assemblies were chosen because they have previously been calculated by the methods currently thought to be the most accurate and which include consideration of resonance scattering and the use of conservative values for $d\nu U^{235}/dE$.* In the previous calculations the steel assembly had exhibited a small calculated critical mass relative to other assemblies. The overpredictions of reactivities were about +1.0% k, +2.7% k, and +2.1% k, respectively. In that study shape factors of 0.94 were assumed in all cases.

The present TDC calculations give shape factors of 0.944, 0.932, and 0.913 for the respective systems. The L/D values are 0.84, 1.17, and 0.69. The overprediction of reactivities for assemblies 32 and 31 are reduced to about +2.5% k and +1.5% k, respectively.

*D. Meneghetti, "Effect of Resonance Scattering on Criticality Calculations of Fast Assemblies," ANL-6466 (December, 1961).

In another study related to the shape factor the values given in ANL-6403* have been re-examined because of a slight discrepancy (~0.5% $\Delta k/k$) between a predicted and a measured (ANL-6544) value. Some errors have been found. The shape factors reported in Table IV of ANL-6403 should be revised as follows:

Reactor I (High density core, high density reflector):
All values lowered by 6.3%.

Reactor II (Low density core, low density reflector):
All values unchanged.

Reactor III (Low density core, high density reflector):
All values lowered by 3.0%.

Reactor IV (High density core, low density reflector):
All values lowered by 3.9%.

The correlation between shape factor and the ratio of the spherical to cylindrical core surface area has been extended to the small, high density, and highly enriched uranium systems. It was found that for all critical systems the following relationship is approximately satisfied in the range of interest ($0.15 < L/D < 2.5$):

$$\text{Shape factor} \approx (A_S/A_C) + 0.1$$

where A_S and A_C are spherical and cylindrical core surface areas, respectively.

2. ZPR-VI and ZPR-IX

a. Building - The search for, and sealing of, cracks around penetrations in Cell No. 4 to minimize air leakage rates is continuing.

b. Cell No. 5, ZPR-VI - Equipment - Approximately 50% of the work for Cell No. 5 (ZPR-VI) is now complete. The matrix tubes have been assembled on both halves of the facility and are being numbered to identify their location. The dual purpose control/safety rod drive mechanisms have been mounted.

The wiring of the bed and table assembly and the dual purpose rod drive mechanisms is in progress. Installation of instrument coaxial cables through the shielding wall is continuing. The closed circuit TV system between Cell No. 5 and the control room has been installed and is being checked out.

---

*W. B. Loewenstein and G. W. Main, "Fast Reactor Shape Factors and Shape-Dependent Variables," ANL-6403 (November, 1961).

3. JUGGERNAUT

During the month of April, the reactor was operated at the design power level of 250 kw in order to check shielding and thermal behavior. The reactor power level was determined by temperature differences and in flow measurements at the heat exchanger.

Shutdown heating in the fuel plates was measured with no water in the core and restricted helium circulation (dump valve closed) to simulate a loss of coolant accident. For a decay heat rate corresponding to operation at 250 kw for 24 hr, the maximum fuel plate temperature reached was 100°C. Shim and control rod temperatures were measured during operation at full power. The values obtained were 160°C and 105°C respectively. The results of these experiments show (as predicted in the reactor hazards analysis) that there are no shutdown heating problems in the fuel or in the control elements during steady-state operation.

The reactor shielding was found to be generally adequate, although spots exist where the radiation leakage is above biological tolerance. Two of these spots are in limited access areas, the reactor top and pump room, which will not normally be occupied during reactor operation so that additional shielding may not be warranted.

The critical experiments on the JUGGERNAUT reactor have been completed. Experimental core physics data were in good agreement with calculated values in all cases. All safety criteria involving physics parameters have been satisfied. A report outlining the startup procedure and tests remains to be written.

B. EBR-I

1. Mark III Operation

Operation of the reactor continued during the month for the purpose of training personnel and the incidental irradiation of materials. Samples were irradiated for Phillips Petroleum Company's Atomic Energy Division. These irradiations are being performed in a program of developing threshold detectors for use in measuring fast neutron flux in reactor test facilities and also in the study of n-p reactions in rare earth nuclides.

Low power operation of EBR-I was also provided for the calibration of a solid state spectrometer for an ANL program.

Approval has finally been received to proceed with the modification to the ventilating system in the EBR-I hot cell. This is to be accomplished prior to the unloading of the Mark III core and the subsequent reloading of the Mark IV fuel. Plans and specifications have been sent out to prospective bidders and construction is scheduled for completion by July 1, 1962.

2. Fabrication of Core IV Fuel

Eighty jacket assemblies are available for final preloading inspections. These 80 are sufficient for completion of the last 62 of the 420 fuel rods required. Hardware for an additional 32 assemblies is available if needed.

After final processing and eddy current inspection, 21 feet of 0.080 in. O.D. Zircaloy-2 instrument tubing (fabricated by the Laboratory) was made available for the assembly operation. Fourteen thermocouple well assemblies were brazed, found leak free (helium mass spectrometer equipment), and delivered for final preloading inspection. A thermocouple well assembly consists of an 0.080 in. O.D. Zircaloy tube sealed at one end and brazed into a Zircaloy sleeve. Of the 14 assemblies brazed, 3 samples will be used for NaK fill tests and for metallographic evaluation of the braze.

The instrument tubing could not be tested on the electromagnetic test equipment customarily used for the inspection of thin wall tubing of larger diameter, so special test equipment had to be constructed for this purpose. After the tubing had been tested by this equipment and carefully radiographed, the 11 best tubes were set aside. Metallographic examinations were undertaken at locations in the remaining tubes which appeared to contain defects worse than any of those which appeared in the selected tubes. The metallography revealed small cracks starting from the I.D. and voids in the wall. It was also discovered that the wall thickness of the tubing was generally in the range of 0.011 in. to 0.013 in. Based on metallographic evidence it was concluded that it was highly unlikely that localized reductions in wall thickness of greater than 0.003 in., either from cracks or voids, existed in the 11 best tubes.

C. EBR-II

1. Reactor Plant

The second primary tank dry heat test was completed and the tank restored to room temperature by April 9. Since that date, final installation work inside the tank and preparations for filling with sodium have been underway.

The purpose of testing the primary tank at elevated temperature was described in ANL-6509 (Progress Report, January, 1962) as follows:

"The heated air test has three objectives: (1) to determine temperature distributions throughout the primary tank for the temperature at which sodium will be introduced into the tank; (2) to verify calculated temperature

drops through the primary tank cover and resulting deflections and rotations at elevated temperature; (3) to check operation of the fuel handling system at an elevated temperature. Although it will not be possible to attain normal operating temperature (700°F) in the primary tank without sodium, it is expected to be possible to reach a temperature of 300°-350°F during this test."

All of the above objectives were appropriately met. In addition, the effectiveness of the primary tank cover beam heaters was established. Some details of the test are described below.

During the heating period, the rate of temperature increase in the tank was maintained generally at or near the maximum rate consistent with prescribed limiting temperature differentials and deflection (movement) differentials of the tank structure. The rate of temperature rise was controlled by varying the total power input to the six electrical immersion heaters. The distribution of heat input was controlled by the varying power input to the individual immersion heaters. Use of three temporary fans to circulate the air within the primary tank helped to minimize undesirable temperature differentials. To follow the heating conditions, 160 thermocouples were read hourly, and structural movements were measured at least once each eight hour period. These readings were supplemented by additional data as dictated by the existing test conditions.

The achievable heating rate usually was limited by temperature differentials within the bottom plate of the tank cover, the maximum permissible differential being taken as 100°F. The sector of the tank cover containing the heat exchanger (relatively remote from the immersion heaters) exhibited the lowest bottom plate temperatures. Temperature variations in the metal in other areas of the tank were of smaller magnitude. The top of the tank was hotter than the bottom, until the shield cooling system was operated. With this cooling, the bottom of the tank increased in temperature more rapidly than the top and eventually levelled out at about thirty degrees above the top temperature.

The temperature differential of greatest interest during the test was that (vertically) across the primary tank cover. With the tank at elevated temperature, as during normal operation, a significant heat loss occurs through the tank cover and its associated nozzles to the biological shield cooling system air. This heat loss is accompanied by production of a temperature differential across the cover structure of such sign as to tend to produce downward bowing of the cover. Such bowing, in turn, tends to tilt the cover nozzles so that the lower ends of mechanisms extending through them into the primary tank tend to move slightly radially outward. A large number of measurements of this temperature differential and the corresponding structural deflections (tilt) were obtained. Approximate

ranges of from 80° to 325°F for the tank cover bottom plate average temperature and from 0° to 80°F in the tank cover average temperature differential were included in these measurements. The measurements indicated the radial rotations, or tilt, of nozzles located at various radii in the cover to be generally less than predicted for the measured temperature differentials. The temperature differentials were found to be as predicted within the accuracy of determination, since as expected, a true steady state condition with an ideal temperature distribution could not be realized. The six primary tank hanger roller assemblies, designed to accommodate thermal expansion of the tank and to maintain the centerline of the tank fixed in position, were determined to function properly.

The effectiveness of the electrical heaters located on the top flanges of the radial beams and the sides of the hex webs of the primary tank cover was also determined. Quantitative data were obtained with the heaters energized at two different power levels. The results showed that significant control over the effective differential temperature of the tank cover and the resultant bowing of the cover will be available at operating temperature if needed.

The fuel transfer mechanisms were operated during the dry heat test. Three complete fuel transfer cycles between the reactor and the storage basket were performed with satisfactory results. During this time the average temperature of the primary tank cover bottom plate approached 290°F, with an average temperature differential in the cover of between 40° and 55°F. The lock mechanisms and the lift mechanism were operated during this testing. Operations inside the primary tank were observed with mirrors and a television camera. No alignment problems were encountered during fuel transfer. Only one storage location of the storage basket was tested because additional work was being done on the basket. However, the one location would show any misalignment between the storage basket and the transfer arm due to movement resulting from the temperature differential in the primary tank cover.

Filling of the seal troughs of the two primary tank rotating plugs was also accomplished during the dry heat test. The sealing alloy, which melts at 281°F, provides the seal between the inert argon gas in the primary tank and the reactor building room air. The seal heating systems which are used to liquify the sealing alloy to permit rotation of the primary tank rotating plugs were checked several times during the heat test. Performance was satisfactory.

Upon conclusion of the dry heat test, installation work inside the primary tank and the reactor plant was resumed. Installation of thermal baffles in the reactor vessel upper plenum has been completed. Work is

progressing on installation of the holddown guide segments for simulating subassembly upper adapters around the periphery of the outer blanket; these have been added to increase the accuracy of positioning the holddown during transfer of peripheral subassemblies. The gripper and holddown mechanisms were fitted with new oil seals, and the main spring assembly was modified to reduce operating forces; the reduction in force enables greater sensitivity in force limit switch actuation. Helium leak testing of primary system components has continued. The reactor vessel cover, EM flowmeters, and the EM auxiliary pump were successfully leak tested. Installation of thermal shields for the wall of the primary tank in the vicinity of the heat exchanger is nearing completion. Nuclear instruments are being installed within the instrument thimbles. All piping for the temporary cold trap system exterior to the primary tank has been completed and installation of the pipe heaters started.

The test of the fuel unloading machine carriage with its full load was successfully completed. The subassembly gripper of the machine is now being tested in sodium. This gripper lifts the subassembly from the storage basket in the primary tank up into the coffin on the carriage. (Movement of the carriage over the interbuilding coffin then provides for transfer of the subassembly out of the reactor building.)

The final report* of the Franklin Institute covering hydraulic studies on the six-tenths scale reactor was completed. This report covers the period July, 1958 through December, 1960.

An automatic control system for possible future use on the EBR-II is being studied. The representation of the reactor kinetics equations with feedback for use on an analog computer has been completed. The feedback model used in this representation assumes there is an automatic flow control in the primary sodium system and it will maintain the desired operating conditions. The results of the analog computer program have been compared with the results obtained from the IBM-704 program. The agreement of results is usually within a few percent.

2. Power Plant

Some progress was made in checking equipment, making minor repairs or modifications, and installing additional devices. Activity in the Power Plant tapered off as manpower was shifted to the Reactor Building.

---

*D. T. Rymsa and G. P. Wachtell, "Flow Model Study of the EBR-II," F-A2201, The Franklin Institute, Philadelphia, Pennsylvania.

The high-level alarms on the Nos. 1, 3, and 4 heaters were tested and electrically reconnected as necessary. The piping to these alarms is being modified to permit quick operational tests to be made. No. 1 is completed, Nos. 3 and 4 await delivery of pipe fittings.

Wiring errors in the startup boiler feed pump loading system were corrected. The system now operates satisfactorily. A writeup was prepared describing the operation of this system.

Attempts were made to repair a leak in the overflow weir of the No. 2 feedwater heater tank. This repair will be tested in the future.

A pressure-regulating valve was installed in the condensate system and a new control valve was installed at the condensate inlet to No. 2 feedwater heater.

A water level gage and a tank drain were installed in the aluminum condensate storage tank. The inside of this tank is being prepared for painting with a vinyl base paint to reduce aluminum corrosion.

3. Sodium Boiler Plant

Helium leak testing of the secondary sodium piping has been completed as far as possible at this time. Three suspect welds have been repaired. The piping between the sodium tank car storage area and the Sodium Boiler Plant and the Reactor Building has been traced with electric resistance heaters, insulated, and made ready for use. The oil heater has been connected to the first railroad tank car to be unloaded and level probes installed. To test out the installation, the oil heater was turned on and the tank brought up to 250°F without difficulty. The superheater startup line has been fabricated and installed.

Insulation, miscellaneous work and continuance work on Package IV continued. Work on sandblasting, painting and coating, along with the installation of inductive heating wire and ferritic steel cladding of stainlesss steel sodium piping progressed.

Sixty-cycle induction heating windings were installed on the sodium header from superheaters to the evaporators. These have been tested at 350°F to balance the coils.

4. Fuel Cycle Facility

A substantial effort is continuing on corrective work and on work which had not been completed by the original construction contractor for the EBR-II Fuel Cycle Facility. Since January 13, the date when work began under the Package IV contract, over 6000 manhours have been expended on this phase of the project.

Open areas, up to 42 inches deep, under the concrete floor in the Air Cell of the Fuel Cycle Facility were found. Since these areas presented possible serious consequences, this deficiency has been corrected. This was accomplished by filling the open spaces with sand and adding grout. Three hundred bags of cement were used in the preparation of the grout.

Other corrective work in progress includes cleaning and lubricating the Argon Cell cranes; regrinding and lapping of gasket surfaces on the large vacuum lock flanges; gasket surface repair and rewelding to seal leaks in the small vacuum lock closures; and repair of leaking shielding window tank units.

One of the three in-cell cranes is now in service; it is being used for the installation of service sleeve plugs. It is anticipated that a second in-cell crane and the first two (of eight) electromechanical manipulators will be in service within the next two weeks. Approximately 20 percent of the wiring and piping associated with the Package IV equipment has been installed. Work is now proceeding concurrently on the completion of the facility, the installation of auxiliary equipment, and the installation of services for the Package IV process equipment.

About one-half of the oil-filled tank units of the shielding windows have been installed. The remotely removable glass sections of the windows have not yet been installed, since it is desirable for training purposes to have these sections installed by remote means.

Construction of control cabinets for the fuel refabrication equipment is nearly complete, and installation is well underway. The furnace in which process materials will be degassed has been installed and is being made leak-tight. The manufacturer has succeeded in reducing the gas leakage around the master-slave manipulator seals from 70 cubic inches per day to about 15 cubic inches per day. This leakage should be satisfactory for the proposed application.

Work was started on the pressure-vacuum system for injection casting and on the installation of the Argon Cell service "feed-through's."

Work continued on high frequency power distribution, compressor discharge header, furnace off-gas system, large transfer lock, transfer cell equipment, and valve cabinets.

The prototype fuel subassembly dismantler, being developed to remove the fuel and blanket elements from a subassembly, has been tested in most of its operations with the exception of the device for removing the fuel elements from the support grid. All of the basic cutting and handling operations were successfully performed on a dummy subassembly and on

a prototype subassembly containing natural uranium. The tests indicate that some components need to be relocated and modified to improve viewing and to improve the ease of operating them with the Mod. 8 manipulators. Design work is in progress to correct these deficiencies.

Continuous air cooling of the fuel bundle is needed to dissipate approximately 1 kw of decay heat during the dismantling operation. Initially, the cooling is by axial air flow, similar to when it is in the transfer coffin. After the outer hexagonal sheath is removed, it must be cooled laterally. A test with air flow perpendicular to the fuel elements, with heat input varying from 1 to 5 kw and air flow from 22 to 132 cu ft/min, is now in progress. Preliminary results indicate that 3 kw of heat can be dissipated with an air flow of 75 cfm with the element temperature not exceeding 430°F. The equipment necessary to provide and distribute this flow can easily be provided within the space limitations of the dismantler and the cell. Work is continuing to improve the uniformity of cooling of elements in various parts of the hexagonal array.

5. Training

The Operational Training Program for technicians, which was recessed for the Dry Heat Test, has not been resumed because of priority work in the Reactor Building.

During the month of April, three groups of supervisory trainees and Power Plant operator trainees, comprising a total of 18 individuals, attended training sessions at the Delray Plant of the Detroit Edison Company and at Argonne, Illinois. Each group spent one week at Detroit, followed by one week at Argonne.

6. Fuel Development

a. Fast Reactor Fuel Jacket Development - During the month, partial deliveries of the following refractory metal tubings were received from commercial suppliers.

Material	Dimensions
Mo	0.156 I.D. x 0.003 in. wall
Mo-0.5 w/o Ti	0.156 I.D. x 0.009 in. wall
Nb-1 w/o Zr	0.257 I.D. x 0.012 in. wall

Evaluation studies are scheduled prior to release of the material for fuel jacketing applications.

The procurement of refractory alloys in various forms is continuing. Some difficulties have developed in procurement of these special alloys. Some suppliers appear to be reluctant to release newly-developed alloy materials for evaluation and test purposes.

7. Process Development

a. Melt Refining Process Technology - Preliminary information has been obtained on the volatilization of various condensable fission products during the melt refining of irradiated EBR-II-type fuel. Two recently completed experiments, each using about seven grams of fuel alloy, show that, at melt refining temperatures as high as 1400°C, negligible volatilization of fission product barium, strontium, zirconium, and ruthenium occurred. The principal activities that condensed on a collector above the melt refining crucible were cesium and iodine.

b. Skull Reclamation Process - A demonstration of the skull recovery process on a 150-gram uranium scale is underway in an argon atmosphere glovebox. The demonstration run has proceeded successfully through the noble metal leaching step and the uranium reduction step. Both steps were carried out in a baffled tungsten crucible. The intermetallic compound precipitation step was successfully carried out in a beryllia crucible. Equipment is being designed for further scale-up to a 2.5-kg-uranium batch size.

Beryllia crucibles, which show promise for precipitation and retorting vessels, will probably require a secondary metal crucible to facilitate remote handling of the mechanically fragile ceramic crucible. Two tests have been carried out with a crucible assembly consisting of an isostatically pressed beryllia crucible in a stainless steel secondary crucible, with beryllia powder tamped in the annulus between the two crucibles to retard liquid metal leakage through cracks that may develop in the beryllia crucible. No visible deterioration of the crucible assembly was evident after these tests in which uranium was precipitated from zinc solution and retorted to dryness. Nearly all of the uranium was easily recoverable from the crucibles after retorting.

An alternative to the melt refining process is being investigated for possible use in the recovery of uranium from stainless steel clad fuel pins. The process, which is a modification of the skull reclamation process, would be used for the recovery of uranium from pins which could not be satisfactorily declad by mechanical means should such a contingency arise. The fates of the constituents of stainless steel have been investigated in preliminary experiments. It was found that iron and nickel were readily removed in the noble metal extraction step of the skull reclamation process. However, a substantial amount of chromium was extracted into the flux phase along with uranium. It appears that multistage contacting would be necessary to obtain a suitable separation of chromium from uranium.

c. Blanket Processing Studies - An important step in the blanket process is the separation of the plutonium-bearing zinc-50 weight percent magnesium supernatant solution from the uranium which has been precipitated by magnesium addition and cooling to 400°C. A phase separation

of 95 percent would eliminate the necessity of a wash of the precipitate. Nine such phase separations by means of pressure siphoning with 500-gram batches of uranium ($\frac{1}{20}$th of full scale) gave 95 to 97 percent separations, with little entrainment of solid uranium.

Direct dissolution of stainless steel clad blanket elements would be desirable in the blanket process if the stainless steel constituents did not substantially affect plutonium recovery and purity. Results of a demonstration run indicate that stainless steel and fission elements, which were added in the appropriate amounts, would have no effect on plutonium behavior. A plutonium recovery of 96 percent was obtained by separation of the supernatant phase from the precipitated uranium, and a total recovery of 99 percent was obtained with the use of a single magnesium wash. In another run in which plutonium was not present, it was determined that chromium and iron would be precipitated with the uranium and thus be separated from the plutonium, but that nickel would quantitatively follow the plutonium.

d. Plutonium Recovery Process - Work on the removal of rare earth fission products from uranium-plutonium fuels by selective extraction into a molten halide flux is being continued. Further results were obtained on the distribution coefficients of uranium, plutonium and rare earths between magnesium-zinc solution and molten magnesium chloride (see Figure 4). The data shown for cerium and praseodymium are from runs made at two different concentrations (tracer and macro levels) of each rare earth and do not show any variation of the distribution coefficient with rare earth concentration. The distribution coefficient of uranium, unlike those of the rare earths, appears to vary with concentration. This effect and the possibility of a similar effect in the case of plutonium are being investigated.

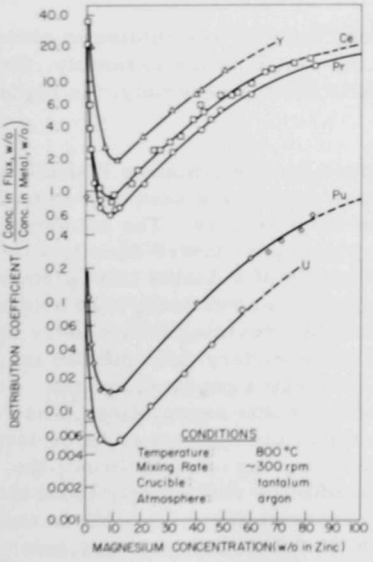

Figure 4. Distribution of Selected Elements between Zinc-Magnesium Alloys and Magnesium Chloride

e. Materials Evaluation - Studies to determine more precisely the effects of flux and zinc-magnesium solutions on beryllia are beginning. In preliminary tests it was noted that the outside surface of a fragment of a previously used beryllia crucible was wetted by a typical processing flux (magnesium chloride-lithium chloride-magnesium fluoride with a small amount of zinc chloride added), while the inside surface of the crucible was not wetted. Two possible reasons for this difference are

(1) grinding of the outside crucible wall during fabrication (which removes the protective coating produced by firing) and (2) density variation in the crucible (the inside of the wall being more dense).

More extensive tests at 800°C in a tungsten crucible have confirmed the good stability of uranium-zinc-magnesium solutions in the concentration ranges of interest for fuel processing.

D. FARET

The general engineering and physics parameters for an experimental facility to test the characteristics of advanced fast reactors have been examined and are described in a report entitled, "Preliminary Proposal for Fast Reactor Test Facility (FARET)," dated April 16, 1962. The report describes in some detail the proposed experimental program in high temperature performance, physics, and dynamics. The cost of the facility is estimated to be $11,033,000. It is currently proposed to construct FARET at the National Reactor Testing Station (NRTS) on the site previously proposed for the ARBOR facility. Existing facilities at EBR-II, approximately 3000 ft northwest of FARET, would be extended and utilized.

1. Core Design

The holddown forces required to keep the fuel assemblies in place in the core are primarily dependent upon the weight of the assembly. Since upflow of coolant is used, the coolant tends to lift the assembly; the higher the flow rate the greater the lift.

Holddown forces have been determined for the tentative FARET fuel assemblies. For a single inlet plenum, these forces are adequate up to the maximum flow rates required for a 50-Mw-50-liter core. The holddown forces, however, are not adequate for use with higher power density subassemblies requiring higher flow rates. The use of a double inlet plenum shown in Figure 5, illustrates a proposed design for retaining high holddown forces on high power density fuel assemblies by providing a secondary inlet plenum operating at lower pressure. The secondary inlet plenum is designed to provide for the large range of flow rates required for the other core components, such as control and reflector assemblies. The double inlet plenum permits the pressure in the inlet plenum to be as large as desired (within the pump capacity) without causing upward thrust; the upward thrust on the high power density assemblies results only from the low pressure in the secondary plenum. By indexing the inlet ports in the assembly holders with appropriate ports in the inlet plenum, many combinations of flow distribution schemes are possible as shown in Table VI.

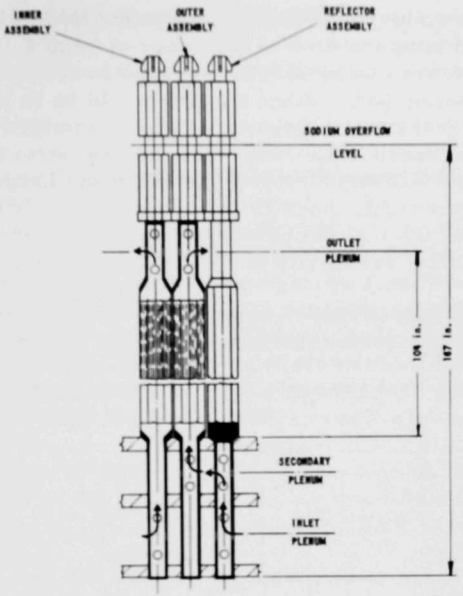

Figure 5. Double Inlet Plenum Possible Flow Scheme

Table VI. Sodium Entrance Schemes

Type of Test	Number of Core Assemblies Connected to Plenum Source	
	Inlet Plenum Pressure < 140 psi	Secondary Plenum Pressure < 45 psi
Uniformly Loaded Core of 50 liters, 52 Subassemblies	52	-
High Performance Test Section in 50-liter Core, 52 Subassemblies	1-7	51-45
Large Uniformly Loaded Core	All Assemblies	-
Zoned Large Core	Inner Assemblies	Outer Assemblies

In connection with the interest in heated zoned critical assemblies, particularly the measurement of phenomena leading to the determination of the Doppler coefficient, an investigation is being continued on the possibility of using electrically heated fuel assemblies. Calculations have

indicated that an electrically heated wire embedded in UO_2 powder will give the required fuel temperatures of the order of 1800°F (1000°C) while the cladding temperature can be held to approximately 250°F (120°C) in a sodium or sodium-potassium bath. Since the UO_2 would be in powder form, it is anticipated that gross fuel expansion will be minimized and possibly eliminated in the powdered UO_2. With the cladding, structural, and coolant maintained at constant temperature, the effect of changes in fuel temperature can be determined. Another important aspect of the electrically heated fuel is that the fuel temperature may be determined from the changes in electrical resistivity of the platinum wire with temperature.

The feasibility of this method will be determined by testing a one-half inch electrically heated fuel element in the laboratory.

III. GENERAL REACTOR TECHNOLOGY

A. Applied Reactor Physics

1. Neutron Scattering

Studies of elastic scattering of fast neutrons from iron, zinc, copper, and U^{235} are proceeding on a continuing basis. The copper and zinc results are shown in Figures 6 and 7, respectively. In both figures the differential elastic scattering cross section is expressed as a series of Legendre polynomials. The mathematical form is given in the Figures. The experimental methods utilize both pulse shape and time-of-flight techniques to discriminate against the inelastic components and the background. Concurrently, inelastic scattering studies of a number of elements, notably Au^{197} and W^{184} (W^{184} is a category I cross-section request), have been conducted along with the elastic scattering measurements.

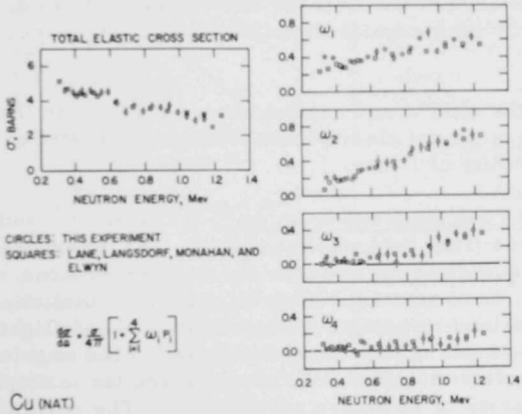

Figure 6

Elastic Scattering of Fast Neutrons from Natural Copper

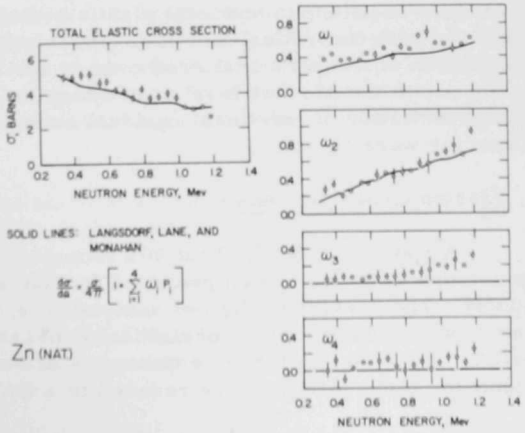

Figure 7

Elastic Scattering of Fast Neutrons from Natural Zinc

A progress report on the recent fast neutron scattering research has been prepared in the form of two papers for presentation at the Summer Meeting of the American Physical Society. The abstracts of these papers follow.

a. Elastic Neutron Scattering from Iron - A pulse-shape discrimination detector has been constructed for the detection of elastically scattered neutrons with energy greater than 500 kev. The detector has excellent gamma-ray rejection. In addition to the pulse-shape discrimination, the detector employs a proportional signal from the photo-multiplier tube which affords good discrimination against inelastically scattered neutrons and the lower energy neutron group from the Li(p,n) reaction. The detector has been used to study the angular distribution of neutrons elastically scattered from iron. Differential cross section measurements were made relative to a carbon standard at 10 angles between 20 and 160 degrees. Measurements were made with a resolution of about 22 kev between 700 and 1100 kev, and with a resolution of about 2.5 kev between 700 and 800 kev. A least squares method was used to fit each angular distribution to a Legendre polynomial expansion.

A comparison of the total cross section measurement with the integral elastic scattering measurement clearly shows the onset of strong inelastic scattering in the vicinity of 1 Mev.

b. The Scattering of Fast Neutrons from Au^{197} - The elastic and inelastic scattering of neutrons from gold was measured. The measurements were made at intervals of about 50 kev over the incident neutron energy $400 \lesssim E_n \lesssim 1400$ kev. Good scattered neutron energy resolution and a low background was obtained by using a pulsed beam time-of-flight technique incorporating an electromagnetic bunching system. The angular distributions of elastically scattered neutrons were corrected for multiple scattering and fitted with a series of Legendre polynomials. The resulting polynomial coefficients and total elastic scattering cross sections were compared with theoretical and other experimental results. The angular distribution of neutrons scattered over to the 77-kev and the 268-kev range together with the 279-kev levels were also measured. The cross sections for the excitation of individual residual nuclear levels by inelastic neutron scattering were obtained.

2. Fission Cross Sections

A sample of Pu^{238}, about 90% isotopically pure, has been procured. Two sample foils have been prepared for use in the gas scintillation fission counter. The heavier of the two sample foils, containing about 200 micrograms, was used to make a preliminary measurement of the fission cross section. By adjusting the time constants in a simple back biased diode circuit the alpha pileups were reduced to a small fraction of the fission

pulse size. However, the fission pulse spectrum remained unacceptably poor, presumably because an appreciable fraction of the Pu^{238} had deposited too close to the edge of the foil. Therefore, only a relative measurement could be made. The results have not yet been completely analyzed, but they show an appreciable fission cross section throughout the energy range from 200 to 1400 kev.

3. Captive Cross Section of Mo^{98}

Monoenergetic neutron capture cross sections have been measured for the mass 98 isotope of the structural material, molybdenum. The cross sections of Mo^{98} are plotted against neutron energies in Figure 8. The rise in the curve near 0.6 Mev is believed to result from interactions with neutrons of angular momentum, ℓ, greater than zero with respect to the target nucleus (probably $\ell = 2$, d-wave). In the absence of such effects, the curve would be expected to drop with the slope of the straight line shown in Figure 8, i.e., with σ proportional to $1/E$.

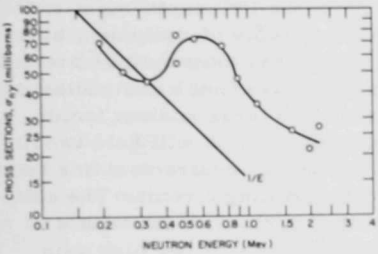

Figure 8. Cross Section of Mo^{98}

4. High Conversion Critical Experiment

Measurements were made of temperature coefficient, flux distribution, and control rod worths in the three-zone core of 3250 elements described in ANL-6544 (Monthly Progress Report for March, 1962). The temperature coefficient was -8×10^5 $\rho/°C$ in the range of 21° to 43°C. Although quite large, this is only about half as large as expected. It is planned to measure void coefficients to determine whether the discrepancy is in moderator worth or in UO_2 temperature coefficient estimate.

Flux measurements included three-dimensional traverses using the following foil materials: dysprosium, gold, Lu^{175}, Lu^{176}, and indium. Both bare and cadmium-covered foils were used in each case. Natural lutetium was used, the two activities being separable by their half-lives. In addition, cadmium ratios in cadmium and manganese were measured near the center of the core.

The traverses indicate there is a saddle-shaped flux pattern, as would be expected, with maxima in the feeder zones.

The core was then changed to a cylinder with a peripheral driving zone. The cylinder (28-cm radius) contained about 2250 fuel elements and had a volume ratio of about 1:3 of H_2O:UO_2. The 9-cm thick peripheral zone contained 800 fuel elements and had a volume ratio of 2.2:1. Unfortunately,

the triangular grid pattern and the reactivity of the two-zone core does not provide a well-defined boundary (i.e., the full four rows, 9-cm thick zone, is too reactive and was compensated for by extending the tightly loaded zone).

A new technique for correcting U^{238} capture distribution for fission product gamma contributions is being tested. The method previously used is unsatisfactory because of variations in fission product decay of foils irradiated in different spectra.

5. ν for U^{235} and Cf^{252}

The data obtained in the initial U^{235} measurements (see Progress Report, December 1961, ANL-6485) in the CP-5 reactor have, for the most part, been analyzed. Based on experience from the U^{235} experiment and on subsequent supplementary experiments, several items of equipment have been redesigned. A four-fold coincidence circuit has been built and tested; this unit is capable of handling pulses of various rise times and widths and lends itself to convenient testing procedures. Two large sodium iodide scintillators have been incorporated in a container which will hold two liters of activated solution. A gamma-gamma coincidence requirement has been established with the aid of a unique count-rate doubling circuit. The calibration counter will consist of a 4π beta system in coincidence with a gamma detector. The 4π beta-detector itself consists of two high gain phototubes viewing the same liquid scintillation sample in a fast coincidence arrangement.

Preparations have been made for the Cf^{252} experiment. A fission chamber, preamplifier, neutron pulse shape detection circuit, and other appropriate electronic equipment such as fast amplifiers and a 100-Mc scaler are ready to be tested.

6. Theoretical Physics

a. Analysis of BORAX-V Lattices (Critical Experiment in ZPR-VII) - Material constants have been calculated for the BORAX-V 1.27-cm square lattice. Thermal constants were obtained using the Sofocate Code. Integral transport theory was used to obtain thermal disadvantage factors. Both free hydrogen and bound hydrogen energy transfer kernels were used. It was found that bound hydrogen hardened the spectrum, compared to the free hydrogen case, so that the cross section for a $1/v$ absorber decreased about 20%. Constants for three fast groups were calculated using the GAM-I code. In this code resonance absorption in U^{238} is treated by the Adler-Hinman-Nordheim technique. Calculations were made using both the P_1 and B_1 approximations with and without self-shielding factors for U^{235} in the epithermal energy range. It was found that: (a) B_1 calculations gave an increase in reactivity of about 1.5% over

P_1 calculations mainly because of the change in the fast diffusion constants; (b) that self-shielding in U^{235} produced little change in reactivity; and that, (c) bound hydrogen decreased reactivity about 1.5% from that obtained with free hydrogen. A material buckling of 11.9×10^{-3} cm^{-2} was calculated for the BORAX-V square lattice. This value appears to be somewhat higher than the experimental value although the sensitivity of the experimental value to reflector savings makes this statement uncertain at the present time.

An investigation of the fast fission factor was made for the BORAX-V 1.27-cm square lattice and the 1.27-cm triangular lattice. A comparison was made of values of ϵ found by using a collision probability transport theory method based on that described by Soodak and Sullivan (NDA-2131-38) and values found from a homogeneous method. It was found that the collision probability method gave values of ϵ-1 about 5% higher than the homogeneous method for the square lattice and about 3% higher for the more tightly packed triangular lattice.

b. Mathematical Numerical Methods Analysis - Some functions of importance to reactor physicists (e.g., the ψ and χ Doppler broadening functions) may be reduced to the error function of a complex agreement, or to the related function:

$$w(z) = e^{-z^2}\left(1 + \frac{2i}{\sqrt{\pi}}\int_0^z e^{t^2}\,dt\right) .$$

Methods of evaluating this function have been reinvestigated. Two continued fraction expansions have considerable merit. The first

$$w(z) = \frac{2i}{\sqrt{\pi}}\,z\left(\frac{1}{(2z^2) - 1} - \frac{2}{(2z^2) - 5} - \frac{6}{(2z^2) - 7} - \cdots \right.$$

$$\left. \frac{4s - 2}{(2z^2) - 2s - 3} - \cdots\right)$$

is rapidly convergent for z in the first quadrant, and $z < 2$. The second fraction,

$$w(z) = e^{-z^2} + i\left(\frac{3\pi^{-1/2}\,z}{3/2 + z^2} - \frac{2z^2/15}{(-2z^2)^{-1} + 1/21} + \cdots \right.$$

$$\left. + \frac{\dfrac{2s\,(2s-1)}{(4s-3)\,(4s-1)^2\,(4s+1)}}{(-2z^2)^{-1} + \dfrac{1}{(4s-1)\,(4s+3)}} + \cdots\right)$$

converges rapidly near the origin. In these expressions, s is the term index. Preliminary trials on the LGP-30 computer indicate that the ranges of practical convergence of the two expressions overlap satisfactorily. Systematic numerical tests are now underway to determine the convergence profiles for various desired occurrences.

c. Fast Reactor Fuel Cycle Studies - The CYCLE production series has continued with studies of the influence of lower fission product removal during reprocessing, higher core and blanket burnups, and the use of niobium instead of stainless steel clad in the core. The uniform linear irradiation core mode and independent zone blanket handling modes have also been studied. These replace the usual cyclic core and blanket mode for fuel management. The influence of a lower density blanket is now being examined.

The next series of CYCLE production problems will return to the Th-U^{233} problems mentioned in earlier progress reports. These problems will be run using ELMOE derived cross sections suitable for the compositions of the various thorium systems.

The CYCLE code is being modified so as to simplify input and also to allow study of the variation across the equilibrium cycle. The modified code will no longer require an initial input tape for the RE 122 (neutron diffusion) portion of the code. All such input will now be written by the code automatically. This change reduces the chance for input errors and also reduces the number of input tapes from two to one.

The input routine has also been made more flexible so that the user may put in regional outer radii, regional volumes, or regional thicknesses. Originally, only the first possibility was permitted. The present change relieves the user of square root or cube root manual operations.

The variation across the equilibrium cycle will use as input the results of a converged CYCLE problem. Either the variation of the core with blanket fixed, or the variation of the blanket with core fixed will be allowed. The principal new input number required is the number of time intervals into which the cycle is to be portioned.

d. Analysis of Scattering Law for Moderators Experiment - Analysis of data obtained from the Scattering Law for Moderators experiment currently taking place at the NRU reactor at Chalk River has been submitted for publication in the Reactor Constants Center Newsletters.

The newsletters list the differential scattering cross section $\partial^2\sigma/\partial E\,\partial\Omega$, and the scattering surface $S(\alpha,\beta)$ for H_2O, D_2O, BeO, and graphite. The cross sections $\partial^2\sigma/\partial E\,\partial\Omega$ are given as functions of the scattered neutron energy and angle for several incident neutron energies

and moderator temperature. The scattering surface $S(\alpha,\beta)$ is listed as a function of the parameters α and β, where α represents the square of the absolute value of the momentum change, and β represents the energy transfer.

Table VII summarizes the incident neutron energies and moderator temperatures for which data have been submitted.

Table VII - Incident Neutron Energies and Moderator Temperatures for Differential Scattering Cross Sections

Moderator	Incident Neutron Energy (ev)	Temperatures, °K
H_2O	0.0355	293, 423
	0.0934	293
	0.1238	423
	0.257	293
D_2O	0.0342	423
	0.0394	293
	0.0968	423
	0.1085	293
Be	0.0372	293
	0.1236	293
BeO	0.9161	293
	0.0980	293
C	0.107	293
	0.181	293

e. Calculations of Doppler Coefficient - The Doppler coefficient has been calculated, using the ELMOE code to obtain the coarse group fluxes for several PuO_2-UO_2 and PuC-UC fueled fast reactors. The temperature-dependent cross sections given by Greebler* for Pu^{239} and U^{238} were used. Core volume fractions were 0.52 sodium, 0.32 fuel, and 0.16 stainless steel, the fuel being assumed to be at full density. Calculations were also made with all sodium removed. The reactivity decrease was calculated for an increase of temperature from 300°K to 2500°K. Results are given in Table VIII.

It is observed that carbide-fueled reactors have a reactivity change about 70% of that for oxide-fueled reactors. The available reactivity change from a normal reactor operating temperature to melting for oxide reactors would be perhaps a third or less the values listed. Since carbide

*P. Greebler, et al., "Calculations of Doppler Coefficient and Other Safety Parameters for a Large Fast Oxide Reactor," GEAP-3646 (May 23, 1961).

reactors would have lower fuel temperatures for the same pin size and power density, the indicated difference between carbide and oxide, would, under these conditions, be at least partially compensated for since the temperature difference between operating and meltdown would be greater. Metal-fueled reactors were found to have a coefficient about 10% of that of oxide-fueled reactors.

Table VIII - Doppler Reactivity Decrease for Increase of Temperature from 300°K to 2500°K

Fuel	Pu^{239}/U^{238} Atom Ratio	Sodium Present	- (% δ k) 300° - 2500°K
Oxide	1/9	Yes	2.63
	1/9	No	1.44
	1/7	Yes	1.81
	1/7	No	0.92
Carbide	1/9	Yes	1.94
	1/9	No	1.11
	1/7	Yes	1.30
	1/7	No	0.63

The 1/7 and 1/9 enrichment ratios correspond to a core size range of 2000 to 3000 liters. It is only in large dilute cores that the Doppler coefficient is large enough to be of importance.

The calculated Doppler coefficient with sodium present is seen to be larger than that with sodium absent by as much as a factor of 2. This is principally due to an increase in low energy flux caused by the moderating effect of the sodium. The effect of the varying sodium content on the low energy fission and capture cross sections has not yet been taken into account.

B. Reactor Fuels Development

1. Corrosion Studies

a. Aluminum Powder Product Tubing - The importance of "as produced" hydrogen in powder product tubing has been indicated in corrosion tests at 290°C. Only 2 of 10 samples of Armour Research Foundation tubing produced from as atomized powder remain in good condition after about four months' exposure to 290°C water. By contrast, all ten samples from the same tubing which had received a one hour vacuum heat treatment at 550°C are in good condition. This heat treatment removes a large fraction of the "as produced" hydrogen.

Hot tensile tests have been performed on the powder product tubing with the results shown in Table IX.

Table IX. Tensile Strength of Aluminum Powder Product Tubing

	Ultimate Tensile Strength
315°C Alloy A288 - ARF - as atomized	7500 psi
	7500 psi
Alloy A288 - ARF - milled 48 hr	9200 psi
	9700 psi
Alloy A288 - ARF - milled 72 hr	11,600 psi
	12,200 psi
Alloy A288 - Torrance Brass Co.	7700 psi
	7200 psi
Alloy 341 - ARF - as atomized	9200 psi
	9600 psi

b. Zirconium Alloys for Superheated Steam - There have been no inspections of corrosion test samples during April. Preliminary X-ray diffraction studies (reflection from films produced after exposures to superheated steam of from 88 to 107 days) revealed no difference in films formed at 540°C and 650°C. Zr-2 w/o Ni-0.5 w/o Fe and Zr-1 w/o Cu-0.7 w/o Fe corrosion products produced identical patterns (probably cubic).

c. Lightweight Alloy for Liquid Mercury - The possible use of titanium alloys for radiator tubing in a nuclear reactor power plant operating on a liquid mercury cycle requires adequate corrosion resistance to mercury in a temperature range between 371° and 538°C. The corrosion behavior of these alloys varies considerably and is also affected by heat treatments. No data on nitrided titanium alloys is available in the literature.

Four titanium alloys: Ti-8 Mn, Ti-2.5 Al-16 V, Ti-7 Al-12 Zr, and Ti-3 Al-5 Cr (all w/o) were nitrogen nitrided. These alloys were selected because of their relatively high resistance to mercury at 371°C in previous tests and their potential as structural materials. The nitrided surfaces were a dull golden color, except in the case of the Ti-7 w/o Al-12 w/o Zr alloy which exhibited a bright brass-colored surface.

Corrosion tests of these nitrided alloys revealed that Ti-7 Al-12 Zr and Ti-2.5 Al-16 V suffered no attack in liquid mercury at 454°C after a 14-day test period. However, Ti-8 Mn and Ti-3 Al-5 Cr alloys showed weight losses of 0.05 and 1.11 mg/cm^2 (average of two samples) respectively under the same test conditions. These weight changes are attributed to the cracking of sharp corners and edges on the specimens during exposure.

2. Ceramic Fuels

a. Uranium-Thorium Sulfide - Following the preparation of a 125 gram batch of fully enriched low temperature uranium monosulfide mixture (see Progress Report, January 1962, ANL-6509), the apparatus was modified to give a maximum capacity of 270 grams per run. No new problems were encountered in preparing these larger batches, which are now being used in the preparation of thermal conductivity and irradiation samples.

Modifications were made in the induction sintering equipment which made it possible to maintain a much more pure sintering atmosphere. US pellets pressed from -100M material, which was homogenized at 1800°C for one hour in argon, sintered to only 83.5% theoretical density in one hour at 1800°C. Consequently, a study was made to see if the particle size was affecting the sintering rate. Fractions of -100, -200 and -300M were used in fabricating pellets which were fired in argon for $4\frac{1}{2}$ hours at temperatures ranging from 1740° to 2030°C. Densification showed an inverse relationship to the particle size, maximum density being first reached by the -325M material at 1740°C, the -200M material at 1800°C and the -100M material at 1900°C. Only closed porosity remained at the maximum densities of 91-92% theoretical. Polished sections indicated that sintering had been accelerated by the presence of a small amount of liquid UOS-US eutectic. Although no analyses were made, past observations allow us to estimate that the bodies ranged from 98% to 99+% US phase, with the remainder being UOS. Higher temperatures served only to increase the grain size with some consolidation of pores but no increase in density. Grain growth in these materials was quite extensive. Average grain size ranged from 51 to 243 microns. Smaller grain size for pressing would seem desirable since liquid-phase sintering is thought to proceed at a rate inversely related to the pore size. Finer material could be produced most easily by using a lower homogenization temperature with an extended soak in preference to extended grinding which is more likely to introduce further contamination.

3. Fabrication Development

a. Fabrication of 2-micron Tungsten Foil - Tungsten foil of approximately 2 microns thickness has been produced. It will be used to complete a series of resonance integral measurements in the ATSR reactor.

After several preliminary rolling operations, using various rolling temperatures and cladding materials, it was determined that room temperature (cold) rolling with intermediate stress relieving proved most effective, especially in thicknesses below 1 mil. The starting material was 6 mil Fansteel sheet.

Cold reduction of the tungsten was done by the pack rolling method, i.e., insertion of the tungsten between two $\frac{1}{16}$ in. thick stainless steel sheets, the lead edges of which were joined by welding. Reductions of 10-15% per pass were taken. A total of approximately 60% reduction was performed between stress relieving operations.

In order to prevent oxidation of the foil during stress relieving at 950°C, the tungsten was spaced between two molybdenum sheets which were jacketed in stainless steel and welded closed. After air cooling to room temperature, the foil was removed and placed in the pack rolling container for further reduction. After each stress relief the foil was rotated 90° from the previous rolling direction.

Using the above procedure the 6 mil tungsten was rolled down to approximately 0.1 mil in thickness. A micrometer is useless in this thickness range and final measurements are made by weighing a piece of foil of known area and calculating the thickness using a measured density value. For this particular foil a thickness of 7.5×10^{-5} inches (approximately 2μ) was obtained.

b. Fabrication of Very Thin Zirconium Isotope Foils - The need for stable Zr isotopes (Physics Division) resulted in a contract with Battelle (BMI) for the reduction of the oxides of $Zr^{90,91,92,94}$ to pure metal by calcium reduction and double iodide deposition on a 5 mil tungsten wire. Upon completion of the conversion by BMI the material was transferred to ANL for foil fabrication.

The "as-received" isotopic material (wire approximately $\frac{3}{32}$ in. diameter x 1 in. long), containing the 5 mil tungsten core wire, was reduced by longitudinal and cross rolling to a thickness of 3 mils. A radiograph located the tungsten wire and diffusion zone and this complete area was removed from the foil.

Further reduction of the remaining foil was carried out by means of pack rolling at room temperature; the foil being contained between two $\frac{1}{16}$ in. thick stainless steel sheets, welded together at the lead end. A final thickness of approximately 2 to 5 microns has been obtained on all the above isotopes by this technique. The rolling direction is alternated by a 90° rotation of the foil within the pack, or envelope. Reductions of 10-20% per pass were used and no intermediate anneals were necessary.

4. Nondestructive Testing

a. Ultrasonic Techniques - A sample network has been constructed to improve the electrical-to-mechanical energy transfer between the sound generator and receiver and the crystal transducer. This network is used

for remote mounting and it provides good power transfer and impedance matching. It consists of a coil and capacitor, both placed across the crystal, and the whole tank tuned to the operating frequency. The coil is also a part of an impedance transformer to match the impedances between the crystal and the transceiver.

A pulse generator which produces a 500 volt pulse with a base duration of 0.06 μsec has been completed. This generator will be used in the search for a practical way to resolve sound signals of very short time separation, which correspond to short distances in materials being tested for flaws, bonds, etc.

b. Neutron Techniques - A first set of resolution data has now been evaluated for most of the direct exposure, photographic neutron imaging techniques. It has been found that as the converter screen thickness is decreased to a certain value the resolution for most of the screen materials tends to improve and then essentially levels off for further decreases in screen thickness. This leveling appears to be due to two factors. One is that the radiation emitted from the converter screen has sufficient energy to spread within the film emulsion, thereby limiting the resolution. The second limiting factor appears to be caused by scatter within the converter and film emulsion which becomes detectable because of the long neutron exposures needed to obtain a reasonable photographic density with many of the slower response thin screen methods.

Most of our previous image sharpness data have been confirmed by these current resolution tests. One significant change is that our present data indicate that the use of a double gadolinium screen exposure method would be preferable to the use of a single gadolinium screen used with a lead intensifier. The double gadolinium screen method yields both better speed and resolution than the lead-gadolinium method. Another change is that the superiority of the gadolinium screen technique for resolution is even more pronounced than our previous data indicated. This method appears to have much greater resolving power than any of our other exposure methods, either direct exposure or transfer. High contrast images of holes separated by appreciably less than 0.001 in. have been resolved by this technique.

An evaluation of a Polaroid camera - lithium-6 scintillator method for detecting thermal neutron images has been made and a report prepared. Since this method is extremely fast and convenient, it is very useful for alignment and preliminary radiographic exposures. However, its usefulness for more general radiographic applications appears limited by the 12 to 15% contrast sensitivity capability of the detection method.

c. Radiographic Techniques - A gamma ray spectrometry method of determining the percent U^{235} in depleted uranium using a 512 channel analyzer computer is being developed. The method uses

normal uranium as a basis for comparison. A highly enriched sample is used to produce the gamma spectrum of U^{235}. The U^{235} spectrum is then stripped from the normal spectrum leaving the gamma spectrum of U^{238}. In this manner the fraction of the U^{235} spectrum needed to completely remove the 184 kev gamma peak from the normal spectrum is determined. The gamma spectrum of depleted uranium with various percentages of U^{235} between zero and normal can then be constructed and compared to samples to be analyzed. Samples of ZPR blanket material are now being analyzed and results will be compared to mass spectrometer analysis.

C. Reactor Materials Development

1. Radiation Damage in Metals

Steel and copper specimens irradiated in CP-5 and EBR-I as reported in the previous report (Progress Report, March, 1962, ANL-6544, p. 42) are ready for mechanical testing. The impact tests on steel must be performed in a cave. The impact machine has been installed in the cave, tested, and calibrated. Impact properties of the unirradiated control material will be measured first.

Counting of the nickel monitoring wires placed in each specimen capsule indicates that burnup of Co^{58} by thermal neutron flux is appreciable. Hence additional data are being obtained to determine thermal flux levels so that appropriate corrections may be made.

The dosimetry capsules containing monitoring foils which were irradiated before the specimens as reported in ANL-6525 (Progress Report, February, 1962, p. 40) have been counted, and the data are being analyzed. Some of the foils used in CP-5 were found to be overexposed at 24 hr. Another set has been loaded for a shorter exposure of 1 hr.

A set of 20-group cross sections for computing spectra has been used to calculate experimentally determined activation ratios in Topsy, Godiva, and a slower ZPR-III assembly. This set has also been used to calculate the attenuation of fission neutrons in water. The results of these calculations are being analyzed to determine whether these cross sections can be used to predict the spectra adequately for radiation damage rate calculations.

D. Heat Engineering and Fluid Flow

1. Double Tube Burnout Studies

The double tube burnout test section, as originally designed, failed during the initial test because differential expansion caused the inner tube to bow against the outer tube (Progress Report, December, 1961, ANL-6485). The section was redesigned to use sapphire spacers to help support the inner tube and prevent buckling.

On the initial high power burnout test of the modified section, the power was interrupted by a burnout trip indication from the outer tube. This was unexpected since the outer tube was operated at a considerably lower heat flux than the inner tube. A second attempt terminated in a similar manner and inspection of the test section revealed that two small holes had been burned through the outer tube. The test section was removed and disassembled and it was found that the inner tube had again buckled against the outer tube. The sapphire spacers that were supposed to prevent contact had disintegrated, apparently from vibration against the outer tube.

A design modification has been initiated that will allow the inner tube to move relative to the outer tube and thereby eliminate the compressive stress induced in the inner tube by differential expansion.

E. Chemical Separations

1. Fluidization and Fluoride Volatility Separations Processes

a. Plutonium Particulate Filtration - Additional measurements have been made of the penetration of filters used in the ventilation systems of facilities where plutonium hexafluoride is handled. The plutonium hexafluoride was released into an air stream containing sufficient moisture to ensure the vapor phase hydrolysis of plutonium hexafluoride to a particulate material (probably PuO_2F_2 or PuF_4). The results to date show that the penetration of this particulate material through two AEC filters placed in series ranges from 0.002 percent to 0.00002 percent.

b. Direct Fluorination of Uranium Dioxide Fuel - The efficiency of a two-step fluorination procedure for the removal of plutonium from a solid solution of uranium dioxide and plutonium dioxide mixed with Alundum is being investigated. The oxide mixture was first exposed to 10 volume percent fluorine at 450°C for four hours, and then exposed to 72 volume percent fluorine at 550°C for six hours. About 96 percent of the plutonium in the solid reaction mixture was removed. By lengthening the treatments at 450°C and 550°C to 10 hours each, the plutonium removal was increased to about 98 percent. The re-use of the Alundum inert bed material in the fluorination of several additions of uranium-plutonium oxide mixtures was investigated. Two experiments were performed in which three separate uranium oxide-plutonium oxide charges were consecutively fluorinated for four hours at 450°C and six hours at 550°C using the same Alundum substrate for each of the two experiments. The resulting residue was further fluorinated for ten hours at 550°C. Plutonium removals of about 98 percent were obtained.

A mathematical analysis of off-gas recycle systems was made in order to guide the design of pilot plant-scale experiments directed toward

optimization of process conditions for the fluorination of larger charges of uranium dioxide pellets. A scheme employing off-gas recycle together with the addition of nitrogen as a fluorine feed diluent appears capable of attaining high fluorine efficiencies. Oxygen is produced in the reaction of fluorine with uranium dioxide. Oxygen concentration in the reactor is maintained at any desired level by diluting the fluorine with nitrogen to control the rate of reaction and by varying the gas recycle rate.

Another run in the current pilot plant series was made in which an 18-inch deep bed of $\frac{1}{2} \times \frac{1}{2}$-inch cylindrical uranium dioxide pellets were completely fluorinated at 500°C. The reactant gases in the present run were more dilute than previously used. The inlet gas was about 10 percent fluorine diluted with nitrogen, and the gas recycle rate was about 20 times the inlet fluorine rate. The overall time of fluorination was 43.5 hours. The overall fluorine utilization efficiency was 77.5 percent. Operation was satisfactory, although partial caking of the bed occurred early in the run. The bed residue at the end of the run was free flowing.

c. Fluid-Bed Hydrolysis of Zirconium Tetrachloride - Improved operation of the six-inch diameter fluid-bed reactor for the hydrolysis of zirconium tetrachloride has been achieved by lowering the bed temperature from 450° to 350°C. The current experiments employed zirconium tetrachloride feed rates of 1.2 and 2.2 kg/hr for periods up to 3.2 hours in duration. Improvement of operation was evidenced by (1) particle growth, (2) reduced quantities of fines, and (3) negligible pressure buildup in the reactor during the runs. All of these factors indicate that a higher percentage of the sublimed tetrachloride feed is being converted to the dioxide on the surface of the bed particles. Equally satisfactory results were obtained with a starting bed of material partly coated with zirconium dioxide as well as with fresh alumina. The off-gas condensate stream contained about 0.005 percent of the zirconium fed during a run indicating very low loss of solids (or passage of unreacted zirconium tetrachloride) from the system through the sintered metal filters.

2. Chemical Metallurgical Process Studies

a. Chemistry of Liquid Metals - Measurements of the solubilities of various elements in liquid metal solvents are being continued. It was found that the solubility of neodymium in liquid zinc may be represented by the empirical equation

(425° to 720°C) Neodymium: $\log$ (weight percent) $= 7.074 - 7126\ T^{-1}$

The solubility of uranium in liquid gallium may be represented by the equation

(343° to 649°C) Uranium: $\log$ (atom percent) $= 6.70 - 8840\ T^{-1} + 1.99 \times 10^{6}\ T^{-2}$.

Attempts by differential thermal analysis to determine the peritectic temperature of the transition of the epsilon phase to the delta phase in the uranium-zinc system were unsuccessful. It is believed that the differences in the structures of the phases in the region of the peritectic are very small and, consequently, the heat of reaction is also small. A liquidus temperature of 957° ± 1°C was observed for a 28 percent zinc-uranium alloy.

The solubility of uranium in liquid magnesium-zinc solutions has been measured at 650°, 700°, and 750°C. The data obtained, together with values of the solubility of uranium in pure magnesium derived by extrapolation of the solubility data, are given in Table X.

Table X. Solubility of Uranium in Magnesium-Zinc Solutions

Magnesium Conc. (a/o)	Uranium Solubility (a/o)		
	650°C	700°C	750°C
40	1.40	1.55	1.95
60	0.173	0.203	0.245
80	0.012	0.018	0.021
100	4.3×10^{-4}[a]	9.9×10^{-4}[a]	1.3×10^{-3}[a]

[a]Solubilities obtained by extrapolation of data at lower magnesium concentrations.

In preliminary experiments with the recording effusion balance, several compounds in the calcium-zinc system were observed. A compound having the composition $CaZn_2$ was found. A phase $CaZn_{\sim 5}$, which may have a composition range, was also observed. A new compound $CaZn_{\sim 11}$ was also found. The existence of this compound was confirmed by X-ray analysis.

b. Metal Distillation Studies - In additional runs in the large-scale cadmium distillation unit, the power input was gradually increased to determine the capability of the unit and to uncover problems associated with high distillation rates. The apparent rate of cadmium evaporation reached 102 kilograms per hour, but there was evidence of extensive entrainment of liquid in the vapor.

c. Calorimetry - A preliminary value of -167.20 ± 0.20 kcal/mole has been obtained for the standard heat of formation of $CdF_2(c)$. This may be compared with presently accepted values of -161.2 to -167 kcal/mole. The preliminary value for the standard heat of formation of $MgF_2(c)$ is -265.38 ± 0.70 kcal/mole, which may be compared with the presently accepted value of -264 ± 4 kcal/mole.

Preparations are being made to resume calorimetric combustion of uranium in fluorine. A scheme for analyzing for the products of the combustion and the unreacted uranium has been developed. The calorimetric system is being calibrated.

Exploratory experiments on the combustion of carbon in fluorine have been made. From 0.1 to 1 percent C_2F_6 was formed in the combustion. This amount of hexafluoroethane would introduce an uncertainty of about 0.05 percent in the heat of formation of CF_4. Attempts are being made to improve the combustion technique.

3. General Chemistry and Chemical Engineering

a. Fluid-Bed Calcination Studies in Small-Diameter Columns - The effect of the operating variables of bed temperature and starting particle size on bed particle size is being investigated in the $2\frac{1}{4}$-inch diameter fluid-bed calciner at temperatures of 425°C and 450°C. Relatively coarse starting beds were employed in these experiments, 200 g of -20 +40 mesh and 125 g of -40 +80 mesh aluminum oxide. One molar aluminum nitrate solution is being used as the feed. The feed rate and air-to-liquid volume ratio are being held constant at values of 18 ml/min and 820, respectively. Results showed growth of the coarse fractions as well as an increase in the fines fraction. Excessive "unloading" of fines from the filters and their subsequent return to the bed causes caking of the bed. It is believed that this may be corrected by improvement of the filter blowback cycle.

IV. ADVANCED SYSTEMS RESEARCH AND DEVELOPMENT

A. Argonne Advanced Research Reactor (AARR)

Further studies of plant layout and equipment arrangement have resulted in significant revisions to the original design shown in ANL-6451.* A sub-basement has been added to the reactor containment building, and all primary system heat exchangers, pumps, purification and degasification equipment have been relocated into the sub-basement. The fuel handling and storage canal has also been moved to a position inside the containment building. The equipment building to the north of the containment building, in which the above equipment and a major part of the canal were formerly located, has been converted to a high-bay experimental mockup area. These changes offer significant cost advantages to the over-all plant.

Earlier designs for AARR specified the use of an aluminum-clad, Al-U_3O_8-cermet core. This core contained 6.5 kg of fully enriched U^{235}, and had an operating life of about 10 days. The reference core has now been changed to use stainless steel-clad, UO_2-stainless steel matrix fuel type. With an initial U^{235} content of 84 kg, this core could have an operating life as long as 180 days. Although the cost of fabricating a stainless steel core may be several times that for an aluminum core, the drastic reduction in the number of cores required for a given operating period will yield a sizeable advantage, both economically and with respect to operational procedures. Moreover, the reduction in the number of spent cores stored at any given time in the canal for cooling improves the safety and reliability of the facility.

The use of a heavily loaded core to achieve long core life has certain other benefits. These stem from the harder neutron energy spectrum, which reduces the effective cross-section of Xe^{135} and Sm^{149}. It has been determined that in the proposed new core it is possible to recover from a complete reactor shutdown within three hours by addition of only 1% in reactivity over the condition existing prior to shutdown. Toward the end of core life, when the U^{235} has been burned down to about 50 kg, such recovery is still possible within 30 minutes after shutdown. Thus it appears that despite the long core life, periodic scheduled shutdowns for sample removal and other experimental modifications will be possible. Moreover, the requirements for special emergency equipment to prevent unscheduled shutdowns, which might necessitate core replacement before the end of life, are materially reduced.

In the new 84 kg core, the median energy of fission is 20 ev, whereas toward the end of core life (50 kg core) the median energy is 1 ev. However, since about 40% of the fissions occur below 0.4 ev and about 40% occur above 100 ev, the large shift in median energy actually reflects only a small change in spectrum over the core life.

*D. H. Lennox, et al., "Status Report on the Argonne Advanced Research Reactor," ANL-6451 (November, 1961).

Preparations are therefore being made to perform a second set of critical experiments to investigate stainless steel alloy cores. The critical measurements will be performed in the cell used previously for the ZPR-II and ZPR-V programs. The instrumentation and control circuitry for the assembly has been specified and partially installed. A layout of the core, representing a compromise between the layout planned for the actual reactor and the requirements for simplicity and versatility, characteristic of zero power experiments, has been made. Fuel assembly design offering rigidity, water tightness, and simple means of changing core compositions, are being investigated; prototype models which have promise have been constructed.

United Nuclear Corporation, subcontractors for an engineering study and cost estimate for the AARR facility, has completed its initial study of design information supplied by the Laboratory, and has initiated engineering work on the over-all facility arrangement, flow sheets and core design. A new basic core layout concept has been proposed in which the previous square array of fuel assemblies would be replaced by a hexagonal pattern. This change markedly reduces the severe variations in power generation heretofore noted around the central flux trap. However, by using fuel assemblies having a rhomboidal cross-section rather than hexagonal, the entire core can still be fabricated of identically dimensioned fuel plates. A more detailed study of the concept is in progress.

V. NUCLEAR SAFETY

A. Thermal Reactor Safety Studies

1. Fuel-Coolant Chemical Reactions

Studies of the stainless steel-water reaction by the condenser discharge method were resumed. Runs were carried out primarily with 30-mil wire specimens. Results showed that no detectable reaction occurred up to the melting point of 1370°C. Fully melted metal at 1370°C formed fine particles which reacted to the extent of 2.6 to 4.7 percent. Only about 17 percent reaction occurred at initial metal temperatures of 3000°C, in room temperature water.

A simple apparatus was constructed to study the reaction of solid uranium with steam. In this apparatus, steam is passed over uranium cubes supported on a thermocouple. The volume of hydrogen generated by the reaction is measured at various times. Preliminary results indicated that the parabolic rate law describes the uranium-steam reaction over the range from 600° to 1000°C.

Preparations were completed for the fourth series of experiments in TREAT on graphite fuel specimens; the main parameters being studied are the effect of cladding and constraint. The pulsed irradiations are now in progress.

Metal-water experiments were performed in the TREAT reactor on zirconium-uranium alloy fuel plates; the results from these are not yet available. Two experiments were completed on Zircaloy-2 clad fuel pins with a thoria-urania core that had molybdenum wires (~4-mil) interspersed in it. The lower energy run (2600°C peak core temperatures) gave 6 percent zirconium-water reaction; the pin remained intact with some swelling of the clad. The higher energy run (~3600°C peak central core temperature) gave 29 percent zirconium-water reaction; the pin was ruptured and the molybdenum wires in the core were melted.

2. Metal Oxidation and Ignition Studies

Isothermal oxidation experiments have been performed in the "heat-sink" apparatus on the two uranium alloys (1 atom percent aluminum and a 1 atom percent copper-uranium alloy) that showed the greatest variation of ignition temperatures in oxygen. In the "heat-sink" apparatus, the specimen cubes are pressed between large pieces of metal to prevent excessive self-heating during reaction. Oxidation rate data for the 1 atom percent aluminum alloy shows a rapidly increasing rate between 400° and 500°C compared with the rate observed for pure uranium. The oxidation rate for the 1 atom percent copper alloy shows a greater decrease in rate

with time at 600°C than pure uranium. These two observations explain qualitative changes in ignition temperatures of these alloys; an effort will be made to provide a quantitative explanation.

A theoretical treatment of burning propagation velocity for single strips of metal burning in air has been developed. Assuming combustion to be controlled by gas phase diffusion of oxygen and burning propagation to be determined by heat conduction through the metal, reasonable agreement with experimental values is found. This treatment will be the subject of a paper currently being prepared for publication.

Studies of the ignition of spherical zirconium powder indicate the possibility that very short exposures of the powder to air may cause a marked increase (50 degrees) in ignition temperature. Additional studies of this effect are planned.

Apparatus has been completed which will permit the observation of the surface of a plutonium sample during oxidation. The apparatus consists of a Pyrex reaction cell attached to a microscope stage. A pressure sensing device continuously records the oxygen pressure during a run. The decrease in oxygen pressure indicates the extent of the oxidation reaction.

B. Fast Reactor Safety Studies

1. Experimental Meltdown Program

In-pile experiments are being continued in the TREAT reactor to study the important mechanisms producing failure in fast reactor fuel elements and meltdown product motion.

a. EBR-II Elements in the Absence of Sodium - The Series XXX test specimens were prepared and shipped to Idaho for exposure in TREAT. A test specimen in this series is composed of a cluster of seven EBR-II fuel elements contained in a small size hexagonal tube segment. The hexagonal segment restrains the elements in a manner similar to that expected to occur in EBR-II operations. All tests were dry, i.e., performed in the absence of sodium coolant. The first two specimens were fueled with normal uranium. The second two specimens contained a central element of normal enrichment surrounded by stainless steel dummy elements. The third two specimens contained a central fuel element enriched to 6% U^{235} surrounded by six elements enriched to 4.1% U^{235}.

The specimens described above have been subjected to transient pulses in the TREAT reactor during this reporting period. The preliminary results of the tests performed on the four samples are given in Table XI.

Table XI. Series XXX - Dry EBR-II Clusters

Test No.	Estimated T, °C	Fuel in Specimen
1	1040	All normal
2	Thermocouple parted (very high)	All normal
3	>1035	Normal and dummies
4	1100	Normal and dummies
5	930	6% and 4.1% U^{235}
6	~1300	6% and 4.1% U^{235}

2. Equipment Development

a. Dry Opaque Capsule for Remote Assembly - The coffin lower section was shipped to the shop for modification of the lifting ears. A special transformer was wound which can be installed in the interior of the cave where capsule assembly will take place. This arrangement eliminates the necessity for bringing heavy current, conducting leads into the cave.

b. Small (Package) Sodium Loop - The design of the in-cave handling equipment has been started. Construction and wiring of the control instrument consoles is approximately 10% completed.

c. Large TREAT Loop - Construction has started on the tank pit which will house the sodium dump tank. The pit was excavated and lined with concrete. Work continued on the installation of instruments in the control panels for the large sodium loop.

3. Theoretical Studies

A topical report entitled "A Theoretical Study of Destructive Nuclear Burst in Fast Power Reactor," ANL-6512, has been issued. This report describes the calculation of destructive bursts in fast reactors by an improved Bethe-Tait method, which for the purposes of calculation, neglects the propagation of a pressure wave. Then exact numerical calculations for hydrodynamic and neutronic conditions during the power burst are performed in order to assess the importance of neglecting the pressure wave. The salient outcome of this comparison is that the Bethe-Tait method tends to predict, for a given accident, a lower integrated energy yield and a higher pressure than the more accurate numerical calculation.

VI. PUBLICATIONS

Papers

KINETICS OF PARTICLE GROWTH IN A FLUIDIZED CALCINER
B. S. Lee, Ju Chin Chu, A. A. Jonke, and S. Lawroski
A.I.Ch.E. Journal 8 (1), 53 (1962)

NEUTRON CAPTURE CROSS SECTIONS OF ^{236}U
D. C. Stupegia, R. R. Heinrich, and G. H. McCloud
J. Nuclear Energy, Reactor Science and Technology, Parts A/B, 15, 200 (1961)

Abstracts of Papers Presented at the 1962 Spring Meeting of the American Physical Society, Washington, D. C., April 23-26, 1962
Bulletin of the American Physical Society, Series II, Vol. 7, No. 4, p. 334 (1962)

ANALYSIS OF FAST-NEUTRON INTERACTION WITH YTTRIUM, ZIRCONIUM, AND NIOBIUM
P. A. Moldauer

SCATTERING OF FAST NEUTRONS FROM Ta^{181} AND U^{238}
Alan B. Smith

ELASTIC SCATTERING OF FAST NEUTRONS FROM Cu, Zn, Zr, AND Nb
D. Reitmann and A. Smith

ANL Reports

ANL-5781 Addendum (Revision 1) — HAZARDS EVALUATION REPORT ASSOCIATED WITH THE OPERATION OF EBWR AT 100 Mw
E. A. Wimunc and J. M. Harrer

ANL-6055 — THE URANIUM-RICH END OF THE URANIUM-ZIRCONIUM SYSTEM
S. T. Zegler

ANL-6114 — EXAMINATION OF URANIUM-2 w/o ZIRCONIUM EXPERIMENTAL FUEL SLUGS IRRADIATED IN EBR-I
W. F. Murphy, A. C. Klank, and S. H. Paine

ANL-6329 — STATUS REPORT ON LAMB WAVES
Roberta A. di Novi

ANL-6408 HAZARD EVALUATION REPORT ON THE FAST REACTOR ZERO POWER EXPERIMENT (ZPR-III)
R. O. Brittan, B. Cerutti, H. V. Lichtenberger, J. K. Long, R. L. McVean, M. Novick, R. Rice, and F. W. Thalgott

ANL-6480 GAMMA-RAY DISCRIMINATION IN A PROTON-RECOIL PROPORTIONAL COUNTER
E. F. Bennett

ANL-6482 AN ANALOG COMPUTER MODEL OF A MULTIPLE REGION REACTOR
L. C. Just, C. N. Kelber, and N. F. Morehouse, Jr.

ANL-6501 SOME CALCULATIONS PERTAINING TO FAST REACTOR SAFETY
D. M. O'Shea, D. Okrent, and J. M. Chaumont

ANL-6505 AN INVESTIGATION OF ENTHALPY DATA FOR WATER AND WATER VAPOR IN THE CRITICAL REGION
E. S. Nowak and R. J. Grosh

ANL-6508 ON THE EQUATION OF STATE FOR WATER AND WATER VAPOR IN THE CRITICAL REGION
E. S. Nowak and R. J. Grosh

ANL-6511 MULTIGROUP CALCULATIONS OF EFFECTIVE DELAYED-NEUTRON FRACTIONS, PROMPT-NEUTRON LIFETIME, AND RELATED KINETICS PARAMETERS. IBM-704 PROGRAM 1188/RE
L. C. Kvitek

ANL-6512 A THEORETICAL STUDY OF DESTRUCTIVE NUCLEAR BURSTS IN FAST POWER REACTORS
V. Z. Jankus

ANL-6514 EBWR CORE DESIGN STUDIES
H. P. Iskenderian and C. E. Carson

ANL-6523 A STUDY OF LIQUIDS BY NEUTRON SCATTERING
P. J. Persiani

ANL-6524 OPTIMIZATION OF EFFICIENCY OF A CESIUM DIODE CONVERTER
C. K. Sanathanan